Chemical Science

EDGE ARTICLE

View Article Online
View Journal | View Issue

Cite this: *Chem. Sci.*, 2017, **8**, 4795

Variation of the Fermi level and the electrostatic force of a metallic nanoparticle upon colliding with an electrode†

Pekka Peljo, *[a] José A. Manzanares [b] and Hubert H. Girault [a]

When a metallic nanoparticle (NP) comes in close contact with an electrode, its Fermi level equilibrates with that of the electrode if their separation is less than the cut-off distance for electron tunnelling. In the absence of chemical reactions in solution, the charge on the metallic nanoparticle is constant outside this range before or after the collision. However, the double layer capacitances of both the electrode and the NP are influenced by each other, varying as the function of distance. Because the charge on the nanoparticle is constant, the outer potential of the metallic NP and hence its Fermi level varies as the capacitance changes. This effect is more pronounced for small particles (<10 nm) in diluted supporting electrolyte solutions, especially if the metallic nanoparticle and the electrode have different potentials of zero charge. Nanoparticles were found to be more electrochemically active in the vicinity of the electrode. For example, the outer potential of a positively-polarized 2 nm radius NP was predicted to decrease by 35 mV or 100 mV (depending on the electrostatic model used to describe the electric double layer), when the NP moved from an electrode at 1 V (*vs.* its pzc) to the bulk. The force between the equilibrated NP and the electrode is always repulsive when they have the same pzc. Otherwise there can be an attraction even when the NP and the electrode carry charges of the same sign, due to the redistibution of surface charge density at both the NP and electrode surface.

Received 22nd February 2017
Accepted 4th May 2017

DOI: 10.1039/c7sc00848a

rsc.li/chemical-science

Introduction

Recently, nanoelectrochemistry has become a hot topic, as highlighted, for example, by the special issue in Accounts of Chemical Research.[1–6] Much of the focus has been on observing the current response of the nanoparticle (NP) landing on a small electrode. As described in recent reviews, NPs can stick to the electrode, or collide and move back to the bulk. NPs can dissolve upon contact, or they can catalyse electrochemical reactions that are kinetically limited on the substrate electrode, like H_2 or O_2 evolution, H_2O_2 or O_2 reduction, metal deposition, *etc.*[1–8] In this work, classical electrostatic models are used to describe the difference in the Fermi levels of an electrode and single metallic NP immersed in an electrolyte solution as a function of their separation for different values of the NP radius and of the electrode potential. Generally, the Fermi level of the electrode is imposed by an external power supply. Charge transfer between the electrode and the NP is possible when their separation is lower than the cut-off distance for electron tunneling. Thus, when talking of NP collisions with the electrode, no physical contact is actually needed. The kinetics of electron tunneling could be described by, *e.g.*, the orthodox theory and the time-average value of the NP charge would then be evaluated. This kind of stochastic charge fluctuation has been considered for example for nanoscale bipolar electrodes.[9] The average NP charge is a continuous variable which does not exhibit quantized charging effects when the thermal energy is larger or similar to the energy difference between consecutive charge states of the NP (see ESI†). The charge transferred to equilibrate the Fermi levels depends on the NP size, and hence on its capacitance.[10] It is accepted that the NP can have charges of partial electrons as this charge is considered to be a time-average value.

An alternative approach is to consider the NPs as multivalent redox "molecules" with equally spaced, formal redox potentials. The condition of electrochemical equilibrium between an electrode and a solution of NPs and is equivalent to the Fermi

[a]*Laboratoire d'Electrochimie Physique et Analytique (LEPA), École Polytechnique Fédérale de Lausanne (EPFL), Rue de l'Industrie 17, CH-1951 Sion, Switzerland. E-mail: pekka.peljo@epfl.ch*

[b]*Department of Thermodynamics, Faculty of Physics, University of Valencia, c/Dr. Moliner, 50, E-46100 Burjasot, Spain*

† Electronic supplementary information (ESI) available: Finite element model description, justification of model assumptions, schematic descriptions of the Fermi level changes upon NP collision with an electrode, the simulations of double layer capacitance of an electrode calculated with different double layer models, 3D plots corresponding to the contour plots of Fig. 1, the effect on the electrolyte concentration and NP radius on the potential distribution, surface charge density plots on the electrode and NP and their comparison with those calculated analytically in the absence of electrolyte, details of the calculations of the interaction between dissimilar parallel plates, and a further discussion of the approximate analytical expressions for the force between NP and electrode in the presence of electrolyte. See DOI: 10.1039/c7sc00848a

level equilibration. The electrode potential then determines the relative populations of the different oxidation states, and hence the average oxidation state of the NPs in the solution. The average charge number of the NPs in the solution is a continuous variable analogous to the NP charge in our approach. The important point to be stressed is that the Fermi level of the electrons in the NP, analogous to the electrochemical potential of the electrons in a solution containing NPs, is a continuous variable that describes the tendency to exchange electrons in order to reach electrochemical equilibrium with the electrode. The Fermi level of the electrons in the NP is not necessarily equal to the energy of the NP in one of its oxidation states. In a solution of NPs, the transfer of just a single electron from the electrode to one NP in oxidized state z causes a dramatic change in the energy of this NP, but the electrochemical potential of the electrons in the solution does not undergo any dramatic change. The latter is a property of the solution that is equivalent to the electrochemical potential of the electrons in the single NP that we consider in this work.

Any change in the separation distance between the NP and the electrode affects also the capacitance of the NP, driving charge transfer between the two objects to adjust their Fermi levels. This equilibration can take place only when the NP is close enough for the electron tunnelling to occur. The charge of the particle will continue to change until the cut-off distance is reached. After this point, the charge is constant but the outer potential of the NP will change in response to the change in the capacitance. This is clear in vacuum or in air, but the purpose of this article is to show that this effect is also significant in electrolyte solutions, where the electrostatic interactions are screened by the electric double layer. With low supporting electrolyte concentrations typically used in NP impact experiments to avoid aggregation, the Debye length can be several nm, while the cut-off distance for electron tunnelling is shorter (<1.5 nm).[11] Hence, the capacitance of a NP will be higher close to the electrode surface. When the NP moves away from the surface, the Fermi level of the electrons will actually vary even if the NP charge remains constant! Negatively charged NPs will have less negative outer potential (Fermi level decreases), while the Fermi level will increase for positively charged NPs!

Recently, there has been a discussion in the literature whether the dissolution of NPs takes place in one or multiple steps.[7,12–18] For example, Unwin *et al.*[16] have shown experimentally for the first time that large NPs partially dissolve in multiple collision events, and this observation was confirmed by Long *et al.*[17] and White and Zhang *et al.*[18] However, the exact mechanism of the NP collisions and subsequent leaching has not been clarified. For example, these large NPs seem to be consumed in a series of "bites", with the NP dissolving closest to the electrode.[16] However, it is not clear why the NP dissolution does not take place at the outer surface, as the dissolution would be most likely controlled by the mass transfer of dissolved ions away from the NP surface. If this is the case, dissolution events should be terminated by NP diffusion, and more likely by electrostatic interactions, as proposed recently by White and Zhang *et al.*[18] However, the effect of contact electrification was neglected, and the electrostatic effects were not quantified. Further work is required to resolve the exact mechanism.

As stated above, the NP will equilibrate its Femi level with that of the electrode, but this does not mean that the outer potentials will be equal. For example, Ag and Au have different potentials of zero charge of −0.44 V and 0.18 V *vs.* SHE,[19,20] so that at electrode potentials of 0.6 V *vs.* Ag/AgCl, typically used for Ag dissolution on a gold electrode, the outer potential of Au will be *ca.* 0.6 V while the outer potential of Ag will be *ca.* +1.2 V. This difference in outer potentials is due to the contact electrification (when two electrically-neutral metals are connected, electrons from the metal with the lower work function will flow into the metal with the higher work function, resulting in a Volta potential difference),[21,22] modified by solvent–metal interactions and other surface modifications when the metal is brought into contact with the solvent. Trasatti and Lust have comprehensively reviewed this topic.[19] Of course, the additional effects of ligands such as citrate and of the electric double layer affect the apparent potential of zero charge (pzc) of the NP.

Theory

Poisson–Boltzmann equation

An electric double layer forms around any charged object in an electrolyte solution, where this surface charge affects the solvent molecules and the ions in the solution.[23] The Poisson equation

$$\varepsilon_0\varepsilon_r\nabla^2\psi = -\rho \tag{1}$$

relates the electrostatic potential ψ to the local space charge density

$$\rho = \sum_i z_i F c_i \tag{2}$$

where ε_0 and ε_r are the permittivity of vacuum and the relative permittivity. The concentrations of ions follow the Boltzmann distribution

$$c_i = c_i^b \exp\left(-\frac{z_i F\psi}{RT}\right). \tag{3}$$

In a binary symmetric electrolyte ($z_+ = |z_-| = z$) the Poisson–Boltzmann equation (PBE) is

$$\nabla^2\varphi = \kappa^2 \sinh\varphi \tag{4}$$

where $\varphi \equiv zF\psi/RT$ is the dimensionless potential, $\kappa = (2c^b z^2F^2/\varepsilon_0\varepsilon_r RT)^{1/2}$ is the Debye parameter (or reciprocal Debye length), and $c_+^b = c_-^b = c^b$ is the ionic concentration in the bulk solution (where $\psi = 0$).[23]

The Stern modification adds inner and outer Helmholtz planes next to the charged surfaces. The outer Helmholtz layer is the closest approach of solvated ions to the surface, while the inner Helmholtz layer consists of mostly organized solvent dipoles and may also contain some specifically adsorbed ions that have lost their solvation shell. In the absence of specific ion

adsorption, the potential satisfies the Laplace equation $\nabla^2\psi = 0$ within the Stern layer.[23]

Spherical geometry. Capacitance of the isolated NP

The PBE in spherical geometry, $\varphi'' + (2/r)\varphi' = \kappa^2 \sinh\varphi$, lacks a general analytical solution (see ESI†). When the NP is considered as a charged conducting sphere of radius R_{NP} and the term $(2/r)\varphi'$ is approximated by $-(4\kappa/R_{NP})\sinh(\varphi/2)$,[24] the first integration of the PBE yields the relation between the surface charge density and the surface potential $\varphi_{NP} = \varphi(R_{NP})$

$$\sigma \approx \varepsilon_0\varepsilon_r\kappa\frac{2RT}{zF}\left[\sinh\frac{\varphi(R_{NP})}{2} + \frac{2}{\kappa R_{NP}}\tanh\frac{\varphi(R_{NP})}{4}\right]. \quad (5)$$

Hence, the differential capacitance of the isolated NP is

$$C_{NP}(R_{NP}) \approx C_\infty(R_{NP})\left[\kappa R_{NP}\cosh\frac{\varphi(R_{NP})}{2} + \mathrm{sech}^2\frac{\varphi(R_{NP})}{4}\right] \quad (6)$$

where $C_\infty(R_{NP}) = 4\pi\varepsilon_0\varepsilon_r R_{NP}$ is its value in absence of electrolyte. When $\kappa R_{NP} \gg 1$, the areal capacitance $C_{NP}/4\pi{R_{NP}}^2$ reduces to that of Gouy–Chapman, $C_{GC} = \varepsilon_0\varepsilon_r\kappa\cosh(\varphi_E/2)$ where φ_E is the potential at the charged surface.

Including an uncharged Stern layer of thickness δ free of ions, the relation between the potential values at the boundaries of this layer is

$$\varphi(R_{NP}) = \frac{2\delta}{R_{NP}}\left[\kappa(R_{NP}+\delta)\sinh\frac{\varphi(R_{NP}+\delta)}{2} + 2\tanh\frac{\varphi(R_{NP}+\delta)}{4}\right] + \varphi(R_{NP}+\delta) \overset{\varphi\ll1}{\approx} (1+\delta/R_{NP})(1+\kappa\delta)\varphi(R_{NP}+\delta). \quad (7)$$

The NP capacitance is then obtained from $1/C_{NPS} = 1/C_\delta + 1/C_{NP}(R_{NP}+\delta)$ where $C_\delta = C_\infty(1 + R_{NP}/\delta)$ corresponds to a spherical capacitor of inner radius R_{NP} and outer radius $R_{NP}+\delta$, and $C_{NP}(R_{NP}+\delta)$ is the capacitance of a NP of radius $R_{NP}+\delta$ (*i.e.*, eqn (6) with $R_{NP}+\delta$ replacing R_{NP}).

The capacitance of weakly-charged NPs ($\varphi_{NP} \ll 1$) simplifies to $C_{NPS}^{\varphi\ll1} = C_\infty[1 + \kappa R_{NP}/(1+\kappa\delta)]$. For a NP of radius $R_{NP} = 2$ nm in a 1 : 1 aqueous electrolyte of $c^b = 10$ mol m^{-3} ($1/\kappa = 3.03$ nm, $\varepsilon_r = 78$) with a surface potential $RT\varphi(R_{NP})/zF = 50$ mV, and a potential $RT\varphi(R_{NP}+\delta)/zF = 39$ mV at the outer boundary of the Stern layer of thickness $\delta = 0.33$ nm, these capacitances are $C_{NP}(R_{NP}+\delta) = 37.7$ aF and $C_{NPS} = 28.8$ aF, and the areal value is $C_{NPS}/4\pi{R_{NP}}^2 = 0.57$ F m^{-2}. For comparison, the areal capacitance of an electrode (with a Stern layer) at $\varphi_E RT/zF = 50$ mV is $C_E = [1/C_{GC} + \delta/\varepsilon_0\varepsilon_r]^{-1} = 0.28$ F m^{-2}, where $C_{GC} \approx \varepsilon_0\varepsilon_r\kappa\cosh[\varphi_E/2(1+\kappa\delta)] = 0.32$ F m^{-2} is the contribution from the electrolyte solution.

Force on the NP

Once the potential distribution is known, the electrostatic force $\boldsymbol{F}$ on the NP is evaluated as

$$\boldsymbol{F} = \frac{1}{2}\int_{S_1}\sigma\boldsymbol{E}\,\mathrm{d}A \quad (8)$$

where $\boldsymbol{E}$ is the electric field at the NP surface, σ is its surface charge density, and S_1 is the surface just outside the NP.[25]

Interaction between charged parallel plates

An outline of the interaction between plates helps to understand the numerical results for the interaction between a spherical NP and an electrode. The potential distribution at a distance z from a plate with surface potential $\varphi_{NP} > 0$ is

$$\varphi(z) = 4\mathrm{artanh}[\tanh(\varphi_{NP}/4)\exp(-\kappa z)]. \quad (9)$$

The electrostatic contribution to the force density on the plate

$$\frac{1}{2}\sigma_{NP}E(0) = \sigma_{NP}\frac{\kappa RT}{zF}\sinh\frac{\varphi_{NP}}{2} = 2RTc^b(\cosh\varphi_{NP} - 1) \quad (10)$$

is directed towards the solution. The charge density $\sigma_{NP} = \varepsilon_0\varepsilon_r E(0)$ on the plate affects the ionic distribution. The total ion concentration close to the plate is $c_+(0) + c_-(0) = 2c^b\cosh\varphi_{NP}$, larger than the bulk value $2c^b$. The osmotic pressure difference between the plate surface and the bulk, $\Delta\Pi = 2RTc^b(\cosh\varphi_{NP} - 1)$, exerts a force on the plate that compensates the electrostatic one, eqn (10), as it has the same magnitude and opposite direction.

If we place a second metal plate at a distance s from the plate at $z = 0$ their interaction can be attractive, repulsive or null depending on its potential φ_E. If φ_E is equal to $\varphi(s)$ given by eqn (9), the charge density on the plate at $z = s$ is

$$\sigma_E = -\sigma_{NP}\frac{\sinh(\varphi_E/2)}{\sinh(\varphi_{NP}/2)} < 0 \quad (11)$$

and there is no interaction, even though the plates have charges of opposite sign, because the effect on the plate at $z = 0$ due to the plate at $z = s$ is the same as that due to the electrical double layer beyond s, $\sigma_E = \int_s^\infty \rho(z)\mathrm{d}z < 0$.

If φ_E satisfies $\varphi_E > \varphi(s) > 0$, the charge density on the plate at $z = s$ is more positive than σ_E in eqn (11) and the interaction between the plates is repulsive, even though $\sigma_{NP} > 0 > \sigma_E$. On the contrary, if φ_E satisfies $\varphi(s) > \varphi_E > 0$, its charge density is more negative than σ_E in eqn (11) and the interaction is attractive, even though $\psi_{NP} > \psi_E > 0$.

The capacitance matrix formalism of electrostatics[21] can be used for conductors in electrolyte solutions provided that the potentials are small and the PBE can be linearized. When the plates interact at constant charge, their surface potentials decrease with increasing separation s.[26] If $\psi_{E\infty} = \sigma_E/C_{GC\infty}$ and $\psi_{NP\infty} = \sigma_{NP}/C_{GC\infty} > \psi_{E\infty} > 0$ are the potentials at large s, with $C_{GC\infty} = \varepsilon_0\varepsilon_r\kappa$, then the values at finite separation are

$$\begin{pmatrix}\psi_{NP}(s)\\ \psi_E(s)\end{pmatrix} = \begin{pmatrix}\coth(\kappa s) & \mathrm{csch}(\kappa s)\\ \mathrm{csch}(\kappa s) & \coth(\kappa s)\end{pmatrix}\begin{pmatrix}\psi_{NP\infty}\\ \psi_{E\infty}\end{pmatrix}. \quad (12)$$

When the plates interact at constant potential, their charge densities vary with s as

$$\begin{pmatrix}\sigma_{NP}(s)\\ \sigma_E(s)\end{pmatrix} = \begin{pmatrix}\coth(\kappa s) & -\mathrm{csch}(\kappa s)\\ -\mathrm{csch}(\kappa s) & \coth(\kappa s)\end{pmatrix}\begin{pmatrix}\sigma_{NP\infty}\\ \sigma_{E\infty}\end{pmatrix} \quad (13)$$

where $\sigma_{E\infty} = C_{GC\infty}\psi_E > 0$ and $\sigma_{NP\infty} = C_{GC\infty}\psi_{NP} > \sigma_{E\infty} > 0$ are the values at large separations. Eqn (13) implies that the capacitance of a plate is a decreasing function of s, $C_{NP}(s) = (\partial\sigma_{NP}/\partial\psi_{NP})_{s,\psi_E} = \varepsilon_0\varepsilon_r\kappa\coth(\kappa s)$. The charge density σ_{NP} on the plate with higher potential remains positive. However, $\sigma_E(s)$ becomes negative if $\kappa s < \operatorname{arcosh}(\psi_{NP}/\psi_E)$. At even shorter distances, $\kappa s < \ln(\psi_{NP}/\psi_E)$, the normal stress

$$F(s) = \frac{\varepsilon_0\varepsilon_r\kappa^2}{2}\left[\left(\frac{\psi_{NP}+\psi_E}{2\cosh(\kappa s/2)}\right)^2 - \left(\frac{\psi_{NP}-\psi_E}{2\sinh(\kappa s/2)}\right)^2\right] \quad (14)$$

is negative (see ESI†), corresponding to an attraction between plates with $\psi_{NP} > \psi_E > 0$ and charges densities of opposite signs.[27] Repulsion dominates when increasing ψ_{NP} and ψ_E at constant $\psi_{NP} - \psi_E$.

Interaction between NP and electrode in electrolyte solution

The interaction of two spheres in the absence of an electrolyte solution has been described in ref. 21, and the interaction of the sphere and a plate in the absence of an electrolyte is described in the ESI.† For large spherical NPs ($\kappa R_{NP} \gg 1$) and low potentials ($\varphi \ll 1$), the potential energy when the NP and a planar electrode in electrolyte solution have constant potentials at a separation s is[26,28]

$$\begin{aligned}\tilde{W}(s) &= \frac{C_\infty}{4}\left(\psi_{NP}{}^2 + \psi_E{}^2\right)\ln\left(1-e^{-2\kappa s}\right) \\ &\quad + \frac{C_\infty}{2}\psi_{NP}\psi_E\ln\frac{1+e^{-\kappa s}}{1-e^{-\kappa s}} - \frac{C_\infty}{2}\psi_{NP}{}^2 - \frac{C_{GC\infty}A}{2}\psi_E{}^2 \quad (15)\\ &= -\frac{1}{2}\left(C_{NP,NP}\psi_{NP}{}^2 + C_{E,E}\psi_E{}^2 + 2C_{NP,E}\psi_{NP}\psi_E\right)\end{aligned}$$

where in the last step we have introduced the capacitance matrix coefficients. The capacitance of the NP

$$C_{NP,NP}(s) = C_\infty\left[1 - \frac{1}{2}\ln\left(1-e^{-2\kappa s}\right)\right] \quad (16)$$

is a decreasing function of s and differs from C_∞ by less than 1% for $s > 2/\kappa$. Similarly to the case of parallel plates, the charge on the spherical NP varies with s; in particular, when $\psi_{NP} = \psi_E$ the charge $Q_{NP} = C_\infty\psi_{NP}[1 - \ln(1 + e^{-\kappa s})]$ decreases as it approaches the electrode (at constant potentials), but it may also increase with decreasing s when $\psi_{NP} > \psi_E > 0$.

Modifications of the Poisson–Boltzmann equation

A well-known limitation of the PBE is that the ions are considered as point charges, resulting in abnormally high surface concentrations at high polarisations. Cervera *et al.* took into account the steric effects using a modified Boltzmann distribution, which replaces c_i^b in eqn (3) by $c_i^b/[1 + 2v_i\sinh^2(\varphi/2)]$, where $v_i = 2N_A a_i{}^3 c_i^b$ is a packing parameter, N_A is Avogadro's constant, and a_i is the diameter of the solvated ion i.[29–32] Thus, with increasing polarisation, the surface concentration of counterions cannot exceed the steric limit $1/(N_A a_i{}^3)$. Similar expressions were proposed in the 1940s and 1950s by a number of authors, as reviewed by Bazant.[33] The modified PBE becomes then

$$\nabla^2\varphi = \frac{\kappa^2\sinh\varphi}{1 + 2v_i\sinh^2(\varphi/2)}. \quad (17)$$

Additionally, the relative permittivity of the solution can be modified by the electric field, as described for example by the Booth model:[34–37]

$$\varepsilon_r = n^2 + \frac{a}{|\boldsymbol{E}|}L(b|\boldsymbol{E}|), \quad L(x) = \coth(x) - 1/x \quad (18)$$

$$a = \frac{7N_0\mu(n^2+2)}{3\sqrt{73}\varepsilon_0}, \quad b = \frac{\sqrt{73}\mu(n^2+2)}{6kT} \quad (19)$$

where n is the optical refractive index, $|\boldsymbol{E}|$ is the electric field strenght, $N_0 = 3.343 \times 10^{28}$ m^{-3} is the number density of molecules, μ is the water molecule dipole moment, and k is Boltzmann's constant. The dipole moment of water was adjusted to $\mu = 6.6621 \times 10^{-30}$ C m to obtain $\varepsilon_r = n^2 + ab/3 = 78$ in weak fields $|\boldsymbol{E}| < 1$ MV m^{-1}.[37] The potential distribution is obtained from the numerical solution of these equations. Although the finite ion size effects are take into account, the validity of continuum models for the description of the double layer around NPs of 1 nm radius might be questionable. The modified PBE flattens out the oscillations in the space charge density due to the finite size effects of the electrolyte ions, but the overall surface charge on the NP is not expected to be significantly influenced.[21] Simulations of the electrode and NP capacitances in electrolyte solution calculated with different models are shown in the ESI.†

Computational methods

The system shown in Scheme 1 was studied by finite element simulations with COMSOL Multiphysics 5.2a, as described in the ESI.† The NP was simulated as a conducting sphere. All the charged metal surfaces were considered to have a Stern layer of the radius of the hydrated K^+ ion (0.33 nm)[38] free of supporting electrolyte, and the modified PBE was used to calculate the distributions of potential and concentrations of the supporting

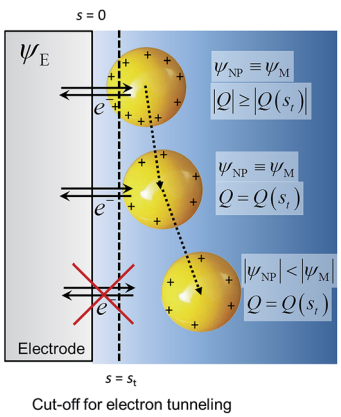

Scheme 1 Nanoparticle potential and charge after collision with the electrode. ψ_E = electrode potential, ψ_{NP} = nanoparticle potential, Q = charge and s = separation from the electrode surface.

electrolyte species. The relative permittivity of the solution was considered to be either constant and equal to that of pure water (model I) or dependent on the electric field intensity as described by the Booth model [model II, eqn (18) and (19)].

All potentials are given with respect to the potential of zero charge (pzc) of the electrode. Thus, for instance, the pzc of the NP is denoted by E_{pzc} and a value $E_{pzc} = 0$ indicates that the NP and the electrode have the same pzc. The electrode and the NP were considered to have the same Fermi level

$$\psi_{NP} + E_{pzc} = \psi_E \quad (20)$$

when their separation was lower than the cut-off distance for electron tunnelling. For example, a NP with $E_{pzc} = -0.5$ V equilibrated with an electrode at its pzc ($\psi_E = 0$) has a potential $\psi_{NP} = 0.5$ V. If the NP moves further away, its charge is constant and equal to the one it had at the cut-off distance for the electron tunnelling. This cut-off distance was arbitrarily chosen as $s_t = 1$ nm; alternatively, it could be calculated, for example, by the Simmons' model.[11,39]

The capacitance of a NP in the vicinity of an electrode differs from that of an isolated NP discussed above because the potential distribution around the NP is affected by the electrode. The differential capacitance $C_{NP} = \partial Q_{NP}/\partial \psi_{NP}$ of the NP was calculated as the function of both the separation distance s and ψ_E. For each value of ψ_E, the NP was first placed at the cut-off distance of electron tunnelling ($s_t = 1$ nm) and was equilibrated with the electrode to obtain the NP charge; its potential $\psi_{NP}(s_t) = \psi_E - E_{pzc}$ was given by eqn (20). For larger NP-electrode separation, $s \geq s_t$, and the same ψ_E, the NP potential ψ_{NP} and the NP differential capacitance C_{NP} were unknown. The NP potential ψ_{NP} was varied from $\psi_{NP}(s_t)$ to slightly lower values and the NP charge $Q_{NP}(\psi_{NP},s,\psi_E)$ was calculated for every value of ψ_{NP}. From these values, $C_{NP}(s,\psi_E) = (\partial Q_{NP}/\partial \psi_{NP})_{s,\psi_E}$ was evaluated and then, the actual value of $\psi_{NP}(s)$ was estimated from the known NP charge, considered to be constant after the NP-electrode collision, that is, $Q_{NP}(\psi_{NP}(s),s,\psi_E) = Q_{NP}(\psi_{NP}(s_t),s_t,\psi_E)$.

The differential capacitance of the electrode was firstly evaluated for a planar surface in 1D geometry, considering the different models for the double layer, and a good agreement with the analytic and numerical results was obtained (see ESI†). Then, the capacitance of the electrode in 2D axis symmetrical geometry was evaluated, showing a good agreement with the 1D simulations.

The Fermi level of the electrons in the NP (and, hence its pzc) varies with the NP size, as shown in a recent review.[40] Additionally, polycrystalline electrode materials have patches with different pzc values,[21] which may also affect the exchange of electrons with the NP. For simplicity, these effects are not considered in this paper.

Results and discussion

Potential and capacitance of the NP (same pzc as electrode)

The potential difference between the NP and the electrode after a collision as a function of the increasing separation distance, the electrode potential and the NP radius are shown in Fig. 1A–C. The differential capacitance $C_{NP} = \partial Q_{NP}/\partial \psi_{NP}$ is shown in Fig. 1D–F (for 3D plots see Fig. S3 in the ESI†). In the case of constant ε_r (model I), the differential capacitance of the electrode increases as a function of potential until no more ions can be packed at the electrode surface, followed by a slow decrease. The comparison with the results of model II, where the relative permittivity varies with the electric field strength, highlights that the capacitance of the NP has a significant effect on the observed behaviour. In model II, the capacitance decreases faster as a function of the increasing potential. Both models produce the famous camel-like dependence of differential capacitance on surface potential,[41] but the decrease of capacitance at higher potentials is less pronounced with constant ε_r. If the capacitance does not significantly vary as the function of the distance from the electrode, there is no change in the NP potential and hence no significant effect on the Fermi level of the electrons in the NP. However, if the capacitance varies significantly, the NP will become less reactive in the bulk. For example, model II predicts a decrease of 20 mV to 35 mV in the NP potential for $R_{NP} = 2$ nm, while model I results in higher potential decrease of 130 mV at 1 V.

Fig. 1 shows that NP radius is another important factor. For $R_{NP} = 10$ nm, model II predicts that the potential changes only

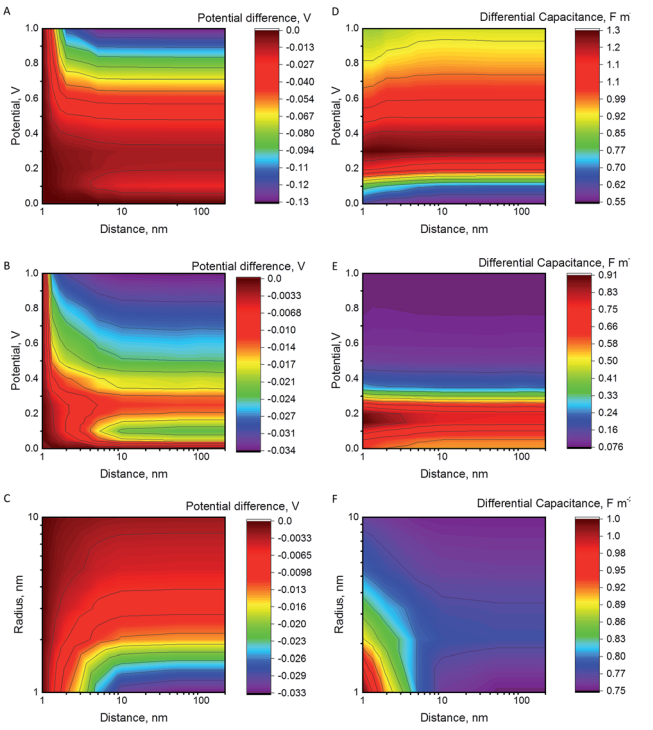

Fig. 1 Potential difference between the NP and the electrode after collision as a function of their separation and of the electrode potential for $R_{NP} = 2$ nm, calculated: (A) with $\varepsilon_r = 78$ (model I) and (B) with the Booth model for the relative permittivity (model II). Differential capacitance as a function of NP electrode separation and NP potential for $R_{NP} = 2$ nm and $E_{pzc} = 0$ V, calculated: (D) with model I and (E) with model II. Effect of the NP radius on: (C) the potential difference and (F) the differential capacitance, calculated with model II and electrode potential of 0.2 V.

3 mV at 0.2 V, in comparison with 35 mV for $R_{NP} = 1$ nm, and for $R_{NP} = 20$ nm the potential decreases by 1.1 mV. If the potential of the electrode is increased to 1 V, the potential decrease for the NP of $R_{NP} = 20$ nm when moving into the bulk is 14 mV, compared to 34 mV for $R_{NP} = 2$ nm. Further increase of the NP radius to 50 or to 100 nm results in a potential decrease of 7 mV and 3 mV, respectively (electrode at 1 V). Hence, slurry electrodes utilizing micrometer sized particles show hardly any effect from the change of the capacitance. This is because the double layer of the electrode perturbs only a small part of the double layer of the large NPs, while this perturbation is larger for small NPs (see Fig. S4 in ESI† to see the electric potential for 2 and 10 nm NPs). If the supporting electrolyte concentration is increased, the thickness of the diffuse double layer decreases, and the effects will be smaller, as shown in Fig. S4C.†

The NPs may contact the electrode and diffuse away. If the NP collision is followed by an electrochemical reaction in the solution, (for example in a system where the electrode is electrocatalytically inert for a given redox couple, while the NP is active), the Fermi level of the NP will equilibrate with the Fermi level of the redox couple in the solution. Interestingly, the NP is most electrochemically reactive (it has more oxidative potential if positively charged, and more reductive potential if negatively charged) close to the electrode surface. While the NP is still close to the surface, the redox reaction with the redox couple in the solution will take place, perturbing the concentration ratio of the redox couple at the NP surface. As the particle moves further from the electrode surface, its Fermi level will change, and the redox reaction can proceed to the opposite direction as a response for this change. Of course, it should be considered whether the process is controlled by kinetics or by mass transfer.

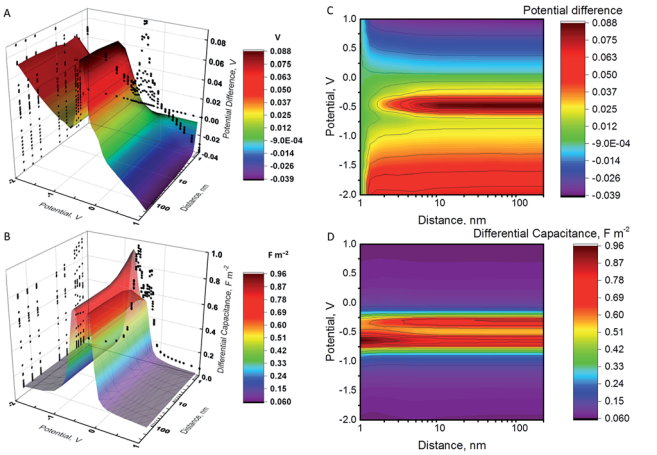

Fig. 2 (A) and (C) Potential difference between the NP and the electrode after collision. (B) and (D) Differential capacitance of the NP. All results have been calculated using model II for $R_{NP} = 2$ nm and $E_{pzc} = -0.5$ V, and are presented as a function of the NP-electrode separation and of the electrode potential.

Potential and capacitance of the NP (different pzc values)

When a NP and an electrode with different pzc values, and hence different (real) chemical potentials of the electrons, get in contact, their Fermi levels equilibrate through contact electrification. A charge transfer takes place from the material with a lower work function into the material with a higher work function. This leads to a situation where the two different materials have the same Fermi level but different electrostatic (or outer) potentials. The changes in the differential capacitance of the NP can then be more drastic, as shown in Fig. 2.

In Fig. 2, we have considered a value $E_{pzc} = -0.5$ V which is actually close to the situation of AgNPs with a glassy carbon or a Au electrode, as Ag has a pzc of *ca.* −0.7 V *vs.* GC and −0.6 V *vs.* Au.[19,20,42] The largest shifts in potential when moving the NP from the vicinity of the electrode into the bulk are observed close to the pzc of the NP. Interestingly, the sign of the change in the potential of the NP changes at electrode potentials slightly above 0 V. Below these potentials, the NP potential increases when it moves to the bulk, with the maximum of *ca.* +90 mV close to the pzc of the NP. When $\psi_E > 0$, $\psi_{NP} - \psi_E$ is negative and increases in magnitude when the NP separates from the electrode. The differential capacitance curve shows an asymmetric shape close to the electrode, with the maximum on the negative side of the pzc value, while the symmetry is recovered in the bulk.

Additionally, the capacitance of the electrode changes when the NP moves farther away from its surface. However, this effect is significant only with very small electrodes, and this double layer perturbation is compensated by the change in the electrode capacitance during the approach, although the magnitude of the change depends on the NP potential when it approaches the electrode. Generally, the baseline of the measured current response in impact experiments shows some variations. This paper suggests that some of these variations could be ascribed to the changes in the capacitance of the electrode due to the NPs perturbing the electric double layer of the electrode, but careful comparison of the experiments with and without NPs would be required. The behaviour of NPs approaching and colliding with the electrode is summarized in the Scheme 2, as well as in Schemes S1 and S2† for the cases where the metals have the same pzc.

Electrostatic force on the NP

The electrostatic force on the NP has been calculated at a separation of 1 nm from the Au electrode for different values of its pzc (Fig. 3A and B). In principle, repulsion when NP and electrode have potentials of the same sign, and attraction when they have different sign, could be expected. However, the discussion on the interaction between dissimilar parallel plates in the Theory section has evidenced that the charge densities on the conductors that interact at constant potentials vary with their separation, and one of them can even reverse sign. Moreover, in the NP-electrode interaction, the charge density is not uniform on the surface of the conductors. The redistribution of charge also contributes to extend the region of attraction slightly on the regions where the NP and the electrode have the same charge sign. The regions of attraction and repulsion between the Au electrode and a AgNP ($E_{pzc} =$

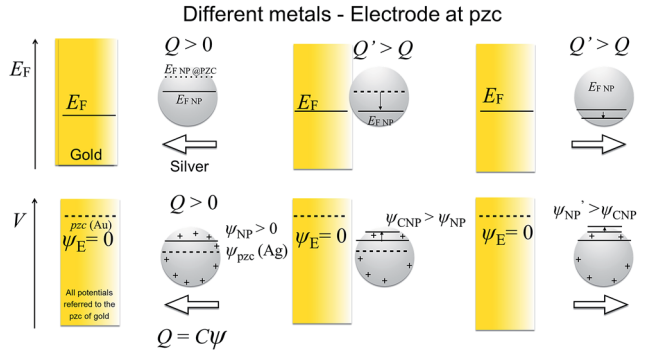

Scheme 2 Electrode and NP made of different metals and the NP has $E_{pzc} = -0.5$ V. Top panel: Fermi levels. Bottom panel: Potential difference between metal and solution. The electrode is at its pzc. Before collision, the AgNP is positively charged ($\psi_{NP} > 0$) and, therefore has a lower Fermi level than at its pzc ($E_{F,NP} - E_{F,NP@pzc} = -e\psi_{NP} < 0$). As the NP capacitance varies with the distance to the electrode, the potential difference between the NP and the solution varies both when the NP approaches the electrode and when departs from it after collision.

−0.5 V) are highlighted in Fig. 3C. The attraction of conductors of dissimilar potentials but of the same sign is known both in the presence[27,43,44] (see ESI† for a detailed explanation) and in the absence[45,46] of electrolyte solutions. Since the electrolyte solution effectively screens the charge and minimizes the charge redistribution, the NP feels the repulsive force after the potentials cross a certain threshold; the behaviour in vacuum is qualitatively different.[45,46] This threshold depends on the pzc difference between the NP and the electrode (Fig. 3B). The charge distributions on the electrode and the NP are shown in the ESI.† This redistribution of charge in either the NP or the electrode close to its pzc leads to a situation where part of the surface has positive charge and part of the surface is negatively charged, and this effect gets stronger with increasing the pzc difference of the two materials.

Fig. 3B shows that pzc difference between the NP and the electrode material will have a significant influence on the electrostatic interaction between the NP and the electrode. Hence, the observed differences of the AgNP oxidation when changing the electrode material from Au to GC[16] could be partly explained by this change in the electrostatic interactions. Fig. 3C shows also that positively charged AgNPs should not be able to approach close enough to the Au or GC electrode to be oxidized upon impact. In reality, the AgNPs are covered with a capping agent like citrate or tannic acid. These capping agents are adsorbed in the inner Helmholtz layer, screen the electrostatic effects of the positively charged core, and in some cases NPs covered with capping agents appear to have a negative charge (as measured with ζ-potential).[7] Additionally, the double layer models used in this work do not consider specific adsorption of ions in the Stern layer.

All these effects add excess negative charge on the AgNP, resulting in attraction with the positively polarized electrode, and oxidation upon impact. However, if the contact with the electrode is enough to make the total charge of the NP positive

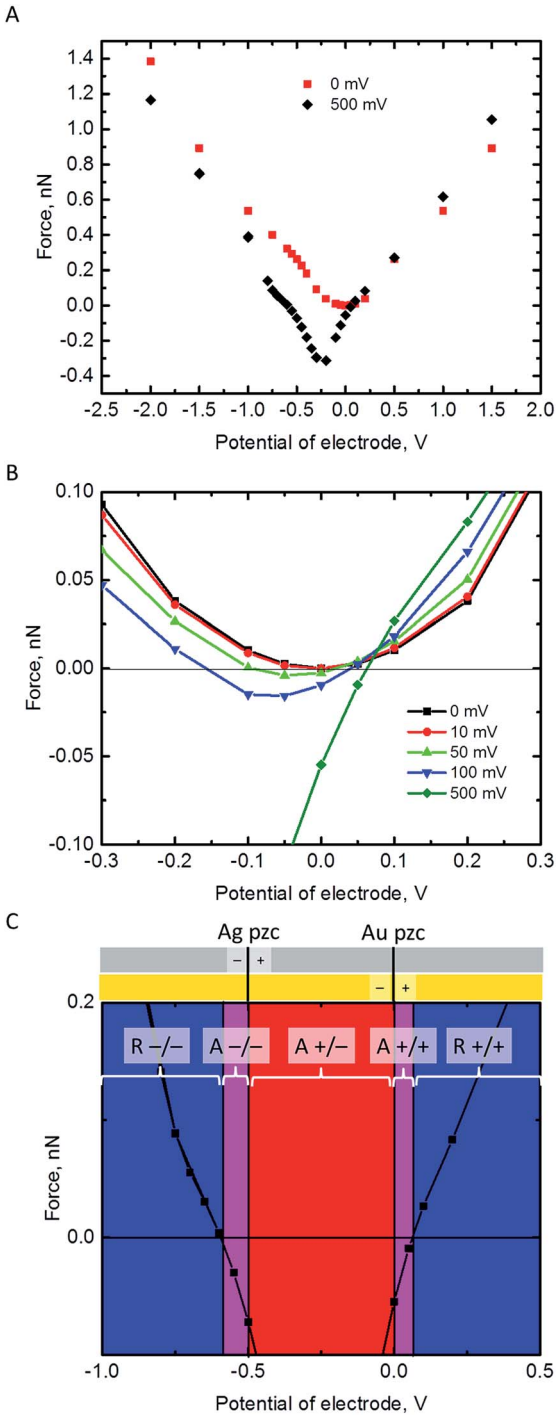

Fig. 3 Electrostatic force on a 2 nm radius NP at a separation $s = 1$ nm from a Au electrode as a function of the electrode potential. The Fermi levels of NP and electrode are equilibrated, $\psi_{NP} + E_{pzc} = \psi_E$, so that the NP potential is higher or equal to that of the Au electrode, $\psi_{NP} - \psi_E = -E_{pzc} \geq 0$. (A) The cases of AuNP ($-E_{pzc} = 0$ mV) and AgNP ($-E_{pzc} = 500$ mV) considered over a wide range of electrode potentials. (B) Effect of the pzc difference on the force over a narrow range of electrode potentials around its pzc. (C) Regions of repulsion (R −/− and R +/+, blue) and attraction (A +/−, red) based on the pzcs of AgNP ($E_{pzc} = -500$ mV) and Au electrode, and the extended region of attraction due to the distribution of charge on the NP and electrode (A −/− and A +/+, violet).

enough so that is feels a repulsive force, then the NP will move away from the surface, resulting in a loss of reactivity as its capacitance decreases.

Conclusions

We have shown that the electric double layer of the electrode increases the differential capacitance of a NP close to the electrode. This means that the outer potential of the NP decreases when the NP moves from the vicinity of the electrode into the bulk (for negative polarization, the outer potential increases). The change in the potential depends on the capacitance of the NP, but also on the size: NPs of above 10 nm radius barely feel any effect, while smaller particles undergo larger changes in potential. However, the effect decreases if higher supporting electrolyte concentrations are used. This means that the NPs are more reactive for oxidation closer to the electrode. For example, 1 nm radius particles will have 30 mV lower potential when moving from the vicinity of an electrode polarized at 0.2 V into the bulk (Fig. 1C). This means also that the surface concentration ratio of the electroactive species will change by a factor of 3. More drastic changes are observed when the NP and the electrode have different potentials of zero charge.

The force between an equilibrated NP and the electrode is always repulsive when they have the same pzc. Otherwise, there is a region of attraction when the NP and the electrode are oppositely charged. However, this region of attraction extends slightly also on the potentials where NP and the electrode have same sign of charge (*i.e.* attraction between two negatively charged or two positively charged objects), because the surface charge redistribution can result in formation of positively charged parts in an overall negatively charged object, and *vice versa*.

In this study, we have used a rather complicated model for the electric double layer, and we expect that the trends of the results will be general. Further improvements could be obtained utilizing more sophisticated methods to describe the double layer structure, and by modelling the electron tunnelling more carefully. However, these results highlight that the effect of the electric double layer of the electrode upon the Fermi level of the NP can be significant, especially with small NPs of different material than the electrode.

Acknowledgements

We would like to acknowledge financial support from the Swiss National Science Foundation, Ambizione Energy, grant 160553. J. A. M. thanks financial support by the Spanish Ministry of Economic Affairs and Competitiveness (MAT2015-65011-P) and FEDER.

Notes and references

1 S. Zaleski, A. J. Wilson, M. Mattei, X. Chen, G. Goubert, M. F. Cardinal, K. A. Willets and R. P. Van Duyne, *Acc. Chem. Res.*, 2016, **49**, 2023–2030.
2 T. J. Anderson and B. Zhang, *Acc. Chem. Res.*, 2016, **49**, 2625–2631.
3 Y. Fang, H. Wang, H. Yu, X. Liu, W. Wang, H.-Y. Chen and N. J. Tao, *Acc. Chem. Res.*, 2016, **49**, 2614–2624.
4 J. Kim, J. E. Dick and A. J. Bard, *Acc. Chem. Res.*, 2016, **49**, 2587–2595.
5 V. Brasiliense, P. Berto, C. Combellas, G. Tessier and F. Kanoufi, *Acc. Chem. Res.*, 2016, **49**, 2049–2057.
6 M. V. Mirkin, T. Sun, Y. Yu and M. Zhou, *Acc. Chem. Res.*, 2016, **49**, 2328–2335.
7 S. V. Sokolov, S. Eloul, E. Kätelhön, C. Batchelor-McAuley and R. G. Compton, *Phys. Chem. Chem. Phys.*, 2017, **19**, 28–43.
8 Y. Wang, X. Shan and N. Tao, *Faraday Discuss.*, 2016, **193**, 9–39.
9 Z. A. Kostiuchenko, B. Zhang and S. G. Lemay, *J. Phys. Chem. C*, 2016, **120**, 22777–22783.
10 M. D. Scanlon, P. Peljo, M. A. Méndez, E. Smirnov, H. H. Girault, M. A. Mendez, E. Smirnov and H. H. Girault, *Chem. Sci.*, 2015, **6**, 2705–2720.
11 C. M. Hill, J. Kim and A. J. Bard, *J. Am. Chem. Soc.*, 2015, **137**, 11321–11326.
12 V. Brasiliense, A. N. Patel, A. Martinez-Marrades, J. Shi, Y. Chen, C. Combellas, G. Tessier and F. Kanoufi, *J. Am. Chem. Soc.*, 2016, **138**, 3478–3483.
13 V. Brasiliense, P. Berto, C. Combellas, R. Kuszelewicz, G. Tessier and F. Kanoufi, *Faraday Discuss.*, 2016, **193**, 339–352.
14 A. N. Patel, A. Martinez-Marrades, V. Brasiliense, D. Koshelev, M. Besbes, R. Kuszelewicz, C. Combellas, G. Tessier and F. Kanoufi, *Nano Lett.*, 2015, **15**, 6454–6463.
15 T. R. Bartlett, S. V. Sokolov and R. G. Compton, *ChemistryOpen*, 2015, **4**, 600–605.
16 J. Ustarroz, M. Kang, E. Bullions and P. R. Unwin, *Chem. Sci.*, 2017, **105**, 1025–1102.
17 W. Ma, H. Ma, J.-F. Chen, Y.-Y. Peng, Z.-Y. Yang, H.-F. Wang, Y.-L. Ying, H. Tian and Y.-T. Long, *Chem. Sci.*, 2017, **129**, 9610–9612.
18 S. M. Oja, D. A. Robinson, N. J. Vitti, M. A. Edwards, Y. Liu, H. S. White and B. Zhang, *J. Am. Chem. Soc.*, 2017, **139**, 708–718.
19 S. Trasatti and E. Lust, in *Modern Aspects of Electrochemistry No. 33*, ed. R. E. White, J. O. Bockris and B. E. Conway, Kluwer Academic Publishers, New York, 1999, pp. 1–215.
20 S. Trasatti, *J. Electroanal. Chem.*, 1971, **33**, 351–378.
21 P. Peljo, J. A. Manzanares and H. H. Girault, *Langmuir*, 2016, **32**, 5765–5775.
22 N. Holmberg, K. Laasonen and P. Peljo, *Phys. Chem. Chem. Phys.*, 2016, **18**, 2924–2931.
23 H. H. Girault, *Analytical and Physical Electrochemistry*, EPFL Press, Lausanne, 2004.
24 H. Ohshima, T. W. Healy and L. R. White, *J. Colloid Interface Sci.*, 1982, **90**, 17–26.
25 J. A. Stratton, *Electromagnetic Theory*, McGraw-Hill Book Company, Inc., New York, 1941.
26 S. Bhattacharjee and M. Elimelech, *J. Colloid Interface Sci.*, 1997, **193**, 273–285.

27 B. V. Derjaguin, *Discuss. Faraday Soc.*, 1954, **18**, 85.
28 R. Hogg, T. W. Healy and D. W. Fuerstenau, *Trans. Faraday Soc.*, 1966, **62**, 1638–1651.
29 J. Cervera, P. Ramírez, J. A. Manzanares and S. Mafé, *Microfluid. Nanofluid.*, 2009, **9**, 41–53.
30 J. Cervera, V. García-Morales and J. Pellicer, *J. Phys. Chem. B*, 2003, **107**, 8300–8309.
31 J. Cervera, *J. Memb. Sci.*, 2001, **191**, 179–187.
32 J. Cervera, J. A. Manzanares and S. Mafé, *Phys. Chem. Chem. Phys.*, 2001, **3**, 2493–2496.
33 M. Z. Bazant, M. S. Kilic, B. D. Storey and A. Ajdari, *Adv. Colloid Interface Sci.*, 2009, **152**, 48–88.
34 F. Booth, *J. Chem. Phys.*, 1951, **19**, 391–394.
35 F. Booth, *J. Chem. Phys.*, 1955, **23**, 453–457.
36 K. Lebedev, S. Mafé, A. Alcaraz and P. Ramírez, *Chem. Phys. Lett.*, 2000, **326**, 87–92.
37 M. Aguilella-Arzo, A. Andrio, V. M. Aguilella and A. Alcaraz, *Phys. Chem. Chem. Phys.*, 2009, **11**, 358–365.
38 E. R. Nightingale, *J. Phys. Chem.*, 1959, **63**, 1381–1387.
39 J. G. Simmons, *J. Appl. Phys.*, 1963, **34**, 1793–1803.
40 M. D. Scanlon, P. Peljo, M. A. Méndez, E. Smirnov and H. H. Girault, *Chem. Sci.*, 2015, **6**, 2705–2720.
41 D. C. Grahame, *J. Am. Chem. Soc.*, 1954, **76**, 4819–4823.
42 H. R. Zebardast, S. Rogak and E. Asselin, *J. Electroanal. Chem.*, 2014, **724**, 36–42.
43 W. B. Russel, D. A. Saville and W. R. Schowalter, *Colloidal Dispersions*, Cambridge University Press, Cambridge, 1989.
44 J. H. Masliyah and S. Bhattacharjee, *Electrokinetic and Colloid Transport Phenomena*, John Wiley & Sons, Inc., Hoboken, NJ, USA, 2006.
45 J. Lekner, *Proc. R. Soc. A*, 2012, **468**, 2829–2848.
46 J. Lekner, *Am. J. Phys.*, 2016, **84**, 474–477.

Chemical Science

CORRECTION

View Article Online
View Journal | View Issue

Cite this: *Chem. Sci.*, 2017, **8**, 5216

Correction: Variation of the Fermi level and the electrostatic force of a metallic nanoparticle upon colliding with an electrode

Pekka Peljo,*[a] José A. Manzanares[b] and Hubert H. Girault[a]

DOI: 10.1039/c7sc90040f

www.rsc.org/chemicalscience

Correction for 'Variation of the Fermi level and the electrostatic force of a metallic nanoparticle upon colliding with an electrode' by Pekka Peljo *et al.*, *Chem. Sci.*, 2017, DOI: 10.1039/c7sc00848a.

The authors regret that the incorrect volume and page numbers were provided for ref. 16 and 17 in the original article. The corrected references are listed below as ref. 1 and 2, respectively.

The Royal Society of Chemistry apologises for these errors and any consequent inconvenience to authors and readers.

References

1 J. Ustarroz, M. Kang, E. Bullions and P. R. Unwin, *Chem. Sci.*, 2017, **8**, 1841–1853.

2 W. Ma, H. Ma, J.-F. Chen, Y.-Y. Peng, Z.-Y. Yang, H.-F. Wang, Y.-L. Ying, H. Tian and Y.-T. Long, *Chem. Sci.*, 2017, **8**, 1854–1861.

[a]*Laboratoire d'Electrochimie Physique et Analytique (LEPA), École Polytechnique Fédérale de Lausanne (EPFL), Rue de l'Industrie 17, CH-1951 Sion, Switzerland. E-mail: pekka.peljo@epfl.ch*

[b]*Department of Thermodynamics, Faculty of Physics, University of Valencia, c/Dr Moliner, 50, E-46100 Burjasot, Spain*

Electronic Supplementary Information

Variation of the Fermi level and the Electrostatic Force of a Metallic Nanoparticle upon Colliding with an Electrode

Pekka Peljo,[a,*] José A. Manzanares,[b] and Hubert H. Girault[a]

[a] *Laboratoire d'Electrochimie Physique et Analytique (LEPA), Ecole Polytechnique Fédérale de Lausanne (EPFL) Rue de l'Industrie 17, CH-1951 Sion, Switzerland.*
[b] *Department of Thermodynamics, Faculty of Physics, University of Valencia, c/Dr. Moliner, 50, E-46100 Burjasot, Spain.*

**Corresponding author.*
E-mail addresses: pekka.peljo@epfl.ch (Pekka Peljo)

1. Model description and justification of assumptions

The potential distribution around a spherical particle with a radius r, separated by a distance s from a center of 1 μm radius disk electrode was investigated in an electrolyte solution containing 10 mM KCl, with the two models as described in the main text. In the aqueous electrolyte solution the particle and the electrode were surrounded by an uncharged Stern layer with a radius of 3.3 Å, where the space charge density is nil. The model was solved in 2D axial symmetry (r = 0 as the axis of symmetry). Additionally, the electric double layer of a planar electrode was investigated with different models, as shown in Figure S1. The obtained results in 1D agreed well with the analytical solutions, and capacitance calculated for an electrode in a 2D axis symmetry agreed well with the results from the 1D calculations.

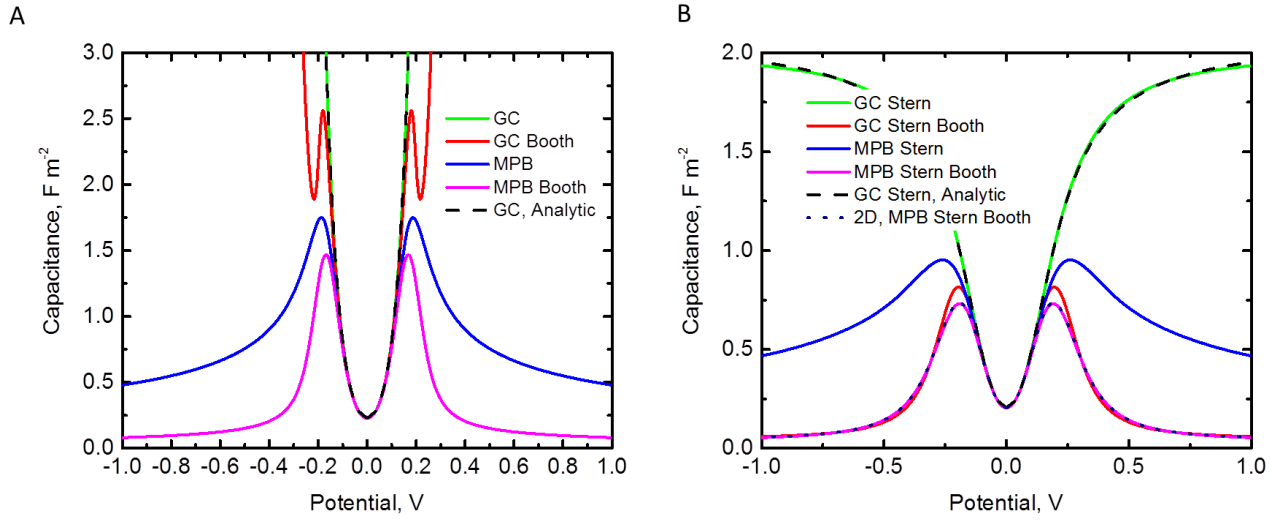

Figure S1. Double layer capacitance of the planar electrode calculated on 1D geometry, A) considering Gouy-Chapman (GC), Gouy-Chapman with Booth (GC Booth) model for relative permittivity of water, modified Poisson-Boltzman model (MPB), also with Booth modification (MPB Booth), and B) Stern modification (δ = 0.33 nm) of all these models. 1:1 electrolyte, 10 mmol L^{-1}.

We have used a modified Poisson-Boltzmann equation that takes into account the finite ion size. This modified Poisson-Boltzmann equation flattens out the electric potential oscillations due to the finite size effects, but the surface charge densities are not expected to be significantly influenced. Moreover, the reliability of continuum models has been studied, e.g., in the context of ion transport through biological ion channels. The comparison of the predictions from the Poisson-Boltzmann equation and from Brownian dynamics has shown that the former are reliable for ion channel radii larger than 1.0 nm.[JA1] Therefore, it is reasonable to accept the validity of the Poisson-Boltzmann equation for the description of the electrical double layer around nanoparticles of radii larger than 1.0 nm.

In this work, the concept of Fermi level equilibration has been applied to the charge transfer between two conductors, the metal NP and the electrode, both immersed in an electrolyte solution. The electrode potential, and hence its Fermi level, is externally fixed by a power supply. The Fermi level is a concept equivalent to the electrochemical potential of the electrons. The electrochemical potential, as the chemical potential, of a species is a thermodynamic quantity that describes the tendency of a system to exchange particles of this species with its surroundings. The energy levels of the particle in the system may also be discrete. *Yet, the chemical potential is not discrete, as it is not necessarily equal to any of the energy*

levels; this is well known in semiconductor electrochemistry. The chemical potential, as the temperature, must be understood as a parameter that determines the probability of occupation of the energy levels of a given species in a system. When the system cannot exchange particles with its surroundings the probability of occupation of the discrete energy levels is only determined by temperature, a continuous variable even though the energy spectrum is discrete. When the system can exchange particles with its surroundings, the probability of occupation of the energy levels is determined by temperature and the chemical potential of the species, both of which are continuous variables. Thus, the equilibration of the chemical potentials of the species in the system and its surroundings is a meaningful concept.

The Fermi level is the electrochemical potential of the electrons in the electrode, $\tilde{\mu}_{e^-}^{E} = -\Phi_E - e\psi'_E$ where is ψ'_E is the electrode potential with respect to vacuum. The Fermi level of the metal nanoparticle in electrolyte solution is $\tilde{\mu}_{e^-}^{NP} = -\Phi_{NP} - e\psi'_{NP}$ where ψ'_{NP} is the nanoparticle potential with respect to vacuum. Although the free energy of the system has not been evaluated, it is implicitly assumed that: (i) it can be considered a function of the nanoparticle charge, $G(Q_{NP})$, (ii) this function can be differentiated with respect to the nanoparticle charge, as if it were a continuous variable, and (iii) the derivative is $-e(\partial G / \partial Q_{NP}) = \tilde{\mu}_{e^-}^{NP} - \tilde{\mu}_{e^-}^{E}$. The condition of Fermi level equilibration is then $\tilde{\mu}_{e^-}^{NP} = \tilde{\mu}_{e^-}^{E}$, or $\psi_{NP} + E_{pzc} = \psi_E$, eqn 20, where ψ_E is the electrode potential with respect to its potential of zero charge (pzc) and E_{pzc} is the pzc of the metal nanoparticle with respect to the electrode pzc. This approach considers the NP as a metallic phase with an outer potential that can vary continuously.

Actually, the NP charge is a discrete variable as it is not possible to exchange a fraction of an electron. This implies that it might not be able to take the value that minimizes $G(Q_{NP})$. In the case we were interested in the electron transfer kinetics, the transfer should be described as a stochastic process according to the orthodox theory.[JA2-JA4] In this theory, the probabilities of electron transfer from the nanoparticle to the electrode, and vice versa, are determined by the free energy changes associated with the transfers, temperature and the tunneling resistance. For a given nanoparticle-electrode separation this theory allows us to evaluate the time average value of the discrete variable Q_{NP}. This time average value is not necessarily one of the discrete values of Q_{NP}.[JA2] At very low temperatures, $k_B T \ll e^2 / 2C_{NP}$, the time average value of Q_{NP} shows the Coulomb staircase. On the contrary, at high temperatures, $k_B T \gg e^2 / 2C_{NP}$, the charge transfer rate is high and the time average value of Q_{NP} is close to the one that makes $G(Q_{NP})$ minimum, $(\partial G / \partial Q_{NP})\big|_{Q_{NP}=Q_{NP,eq}} = 0$. The effects of the discreteness of charge are not seen in this temperature range. The consideration of ψ_{NP} and Q_{NP} as continuous variables is justified by the fact that we do not observe a single NP at a given instant but an average over time.

Alternatively, the consideration of continuous variables can be justified by the fact that we do not observe a single NP but the average behavior of a collection of NPs in solution interacting with the electrode. The NPs are then considered as "molecules" with multiple redox states whose formal redox potentials are equally spaced. The condition of electrochemical equilibrium or Fermi level equilibration for the reaction $NP^z(aq) + e^-(E) \leftrightarrow NP^{z-1}(aq)$, where E stands for metal electrode, is $\tilde{\mu} := \tilde{\mu}_{e^-}^{E} = \tilde{\mu}_{NP^{z-1}}^{aq} - \tilde{\mu}_{NP^z}^{aq}$ or $E = E^\circ_{red(z \to z-1)} + (kT/e)\ln(a_{NP^z} / a_{NP^{z-1}})$, for any *z*. The body of work from

R. W. Murray and others[JA5] demonstrating that electron transfer to small nanoparticles is quantized is related to two facts: (1) $E^{\circ}_{\mathrm{red}(z\to z-1)} \approx E^{\circ}_{\mathrm{pzc}} + (2z-1)e/2C_{\mathrm{NP}}$ is a function of z, and (2) for very small nanoparticles (often, in low relative permittivity solvents) the effective capacitance C_{NP} is so small that the values of the standard redox potentials can be observed individually in a DPV. Since quantized charging seems to be incompatible with the assumption of continuous NP charge, we describe next the conditions under which this assumption is valid.

The NP and the electrode are considered as two systems that reach equilibrium with respect to the exchange of electrons. The negative charge number of the NP is a counter for the number of electrons in the NP. When the charge number is considered a discrete variable, the average value of z is given by

$$\langle z \rangle (T, \tilde{\mu}) = \frac{\sum_z z \exp\{-[\varepsilon(z) + z\tilde{\mu}]/kT\}}{\sum_z \exp\{-[\varepsilon(z) + z\tilde{\mu}]/kT\}}. \tag{JA1}$$

The ratio of probabilities of observing the charge numbers z and $z - 1$ is equal to the ratio of concentrations (or activities) of NPs with these charge numbers

$$\frac{c_z}{c_{z-1}} = \exp\{[\varepsilon(z-1) - \varepsilon(z) - \tilde{\mu}]/kT\}. \tag{JA2}$$

The average charge number can also be evaluated in terms of the electrode potential E. The comparison of eqn (JA2) with the Nernst equation

$$E = E^{\circ}_{\mathrm{red}(z\to z-1)} + (kT/e)\ln(c_z/c_{z-1}) \tag{JA3}$$

evidences the correspondence

$$\varepsilon(z-1) - \varepsilon(z) - \tilde{\mu} = e[E - E^{\circ}_{\mathrm{red}(z\to z-1)}]. \tag{JA4}$$

Assuming a constant NP capacitance, the standard redox potential can be approximated by

$$E^{\circ}_{\mathrm{red}(z\to z-1)} = E_{\mathrm{pzc}} + (2z-1)e/2C_{\mathrm{NP}} \tag{JA5}$$

where E_{pzc} is the NP potential of zero charge (with respect to that of the electrode), which basically arises from

$$\varepsilon(z) = z^2e^2/2C_{\mathrm{NP}} + z(eE_{\mathrm{pzc}} + k) \tag{JA6}$$

and

$$\tilde{\mu} = -eE - k, \tag{JA7}$$

where k is an arbitrary constant. Substituting eqns (JA6) and (JA7) in (JA1), the average value of z can be expressed as in terms of temperature and the electrode potential as

$$\langle z \rangle = \frac{\sum_z z\alpha^z\kappa^{z^2}}{\sum_z \alpha^z\kappa^{z^2}} \tag{JA8}$$

where $\alpha := \exp[-e(E_{\mathrm{pzc}} - E)/kT]$ and $\kappa := \exp(-e^2/2kTC_{\mathrm{NP}})$.

The sum in eqn (JA8) cannot be evaluated analytically but there is an alternative procedure to evaluate the (average) charge number as a function of the electrode potential E which is basically equivalent to a mean field approximation. The NP is considered as an isolated system with a charge $\tilde{z}$; the tilde denotes its continuous character. Similarly to eqn (JA6), the NP energy is $\varepsilon(\tilde{z}) = \tilde{z}^2 e^2 / 2C_{\mathrm{NP}} + \tilde{z}(eE_{\mathrm{pzc}} + k)$. The relation between $\tilde{z}$ and E

$$E = E_{\mathrm{pzc}} + \tilde{z}e / C_{\mathrm{NP}} \qquad \text{(JA9)}$$

is now obtained from eqn (JA7) with the electrochemical potential of the electrons in the NP evaluated from the variation of $\varepsilon(\tilde{z})$ with respect to its number of electrons (i.e., the negative z) as $\tilde{\mu} = -\mathrm{d}\varepsilon / \mathrm{d}\tilde{z} = -\tilde{z}e^2 / C_{\mathrm{NP}} - eE_{\mathrm{pzc}} - k$.

Although only discrete values of the NP charge number are allowed, the average charge number in eqn (JA8) describes the state of the NP solution. In Figure S2, this average value has been represented against $-\ln\alpha$ for different values of $\ln\kappa$ and compared to the continuous charge number in eqn (JA9), here transformed to

$$\tilde{z} = \frac{e(E - E_{\mathrm{pzc}}) / kT}{e^2 / kTC_{\mathrm{NP}}} = -\frac{\ln\alpha}{2\ln\kappa}. \qquad \text{(JA10)}$$

The sum in eqn (JA8) runs over integer values of z and extends from an arbitrary large negative value to a large positive value; the plot in Figure S2 is restricted to a region when the limits of the sum are irrelevant. When the charging energy $e^2 / 2C_{\mathrm{NP}}$ is larger than ca. 2.5 times the thermal energy kT the average charge number shows the Coulomb staircase. On the contrary, the average charge number shows a linear dependence on $-\ln\alpha = e(E_{\mathrm{pzc}} - E) / kT$ when $e^2 / 2kTC_{\mathrm{NP}}$ is lower than 2.5. The mean field or continuous approximation is then very accurate under the latter conditions, while it also predicts the correct slope of the staircase when $e^2 / 2kTC_{\mathrm{NP}} > 2.5$. The NP capacitances involved in this work are relatively large because we are modeling NPs with diameters between 2 nm and 20 nm, in aqueous solution and without taking into account the protecting monolayer as a low-permittivity dielectric shell. The thermal energy kT at room temperature is then larger that the charging energy, $e^2 / 2C_{\mathrm{NP}}$, and therefore it is reasonable to consider the NP charge number as a continuous variable and eqn (JA10) can be used instead of eqn (JA8), as no Coulomb staircase appears under these conditions.

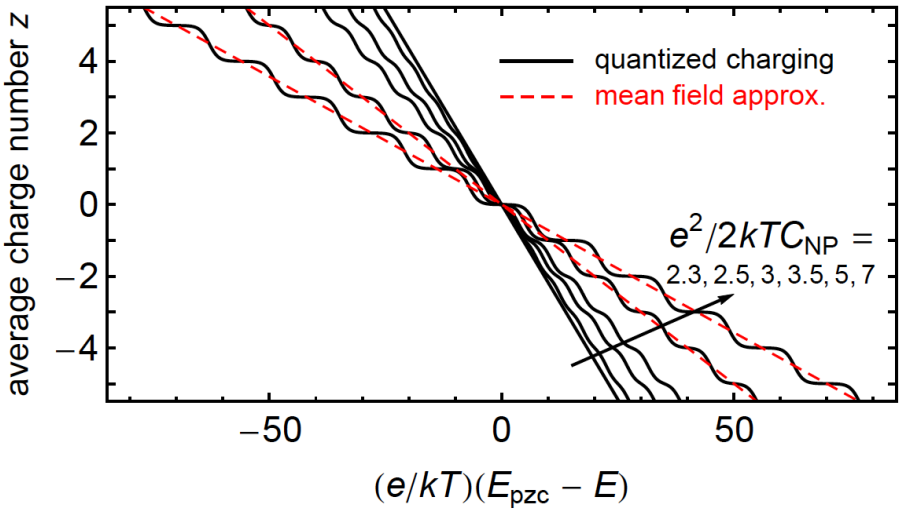

Figure S2. The variation of the average NP charge number with the electrode potential shows the Coulomb staircase when the charging energy $e^2 / 2C_{\mathrm{NP}}$ is a few times larger than the thermal energy kT; the spacing of the ticks in the ordinate scale is one unit. The assumption of the NP charge as a continuous variable is equivalent to a mean field approximation. This approximation is very accurate when $e^2 / 2kTC_{\mathrm{NP}}$ is lower than ca. 2.5. For larger values of this ratio, the mean field approximation (dashed lines, only two are shown for the sake of clarity) does not show the quantized charging but still predicts the correct slope for the variation of charge number with electrode potential.

The restriction to constant NP capacitance has allowed us to clearly establish the conditions under which the average NP charge number does not exhibit quantized charging (i.e. the Coulomb staircase). In most theoretical studies, the NP capacitance is estimated from relatively simple electrostatic models. In this work, the NP capacitance has been calculated from the numerical solution of a modified Poisson-Boltzmann equation that takes into account the finite ion size and the dielectric saturation effect, in addition to the presence of a Stern layer. Obviously, for the purpose of evaluating the differential NP capacitance, the electric charge on the NP must be assumed to be a continuous quantity. Furthermore, when the NP capacitance is not known, the condition of Fermi level equilibration should not be expressed in terms of this capacitance, as in eqn (JA9), but rather in terms of the electric potentials, as in eqn (20), $\psi_{\mathrm{E}} = E_{\mathrm{pzc}} + \psi_{\mathrm{NP}}$.

The electrochemical equilibrium between a metal electrode with fixed $\tilde{\mu}$ and the solution containing NPs is achieved through charge transfer. This transfer changes the concentrations of NPs in different redox states until their fractions are given by eqn (JA2), the Fermi level equilibration condition. Equation (JA2) essentially says that the transfer of a single electron from the electrode to one NP with charge number z causes a dramatic change: the NP is transformed to a reduced state with charge number $z - 1$ and its electrochemical potential changes discretely from $\tilde{\mu}^{\mathrm{aq}}_{\mathrm{NP}^z}$ to $\tilde{\mu}^{\mathrm{aq}}_{\mathrm{NP}^{z-1}}$, with

$$\tilde{\mu}^{\mathrm{aq}}_{\mathrm{NP}^z} - \tilde{\mu}^{\mathrm{aq}}_{\mathrm{NP}^{z-1}} = \varepsilon(z) - \varepsilon(z-1) + kT \ln \frac{c_z}{c_{z-1}}. \qquad \text{(JA11)}$$

Yet, the electrochemical potential of the electrons in the solution of NPs, $\tilde{\mu} := \tilde{\mu}^{aq}_{NP^{z-1}} - \tilde{\mu}^{aq}_{NP^{z}}$ for any z, does not undergo any dramatic change due to this electron transfer. The latter is a property of the solution and not as a property of a single NP. Moreover, $\tilde{\mu}$ is not equal to any of the allowed NP energies given by eqn (JA6) with discrete z. The fact that the electrochemical potential $\tilde{\mu}$ of the electrons in the solution of NPs is a continuous variable makes it possible to make it equal to the electrochemical potential of the electrons in the electrode. The latter statement is valid regardless of whether the Coulomb staircase is observable.

2. Schematic description of the Fermi level changes upon NP collision with an electrode and supplementary figures

Schemes S1 and S2 consider the case of electrode and NP made of the same metal $(E_{pzc} = 0)$, for electrode potential equal ($\psi_E = 0$, Scheme S1) and higher ($\psi_E > 0$, Scheme S2) than the common pzc.

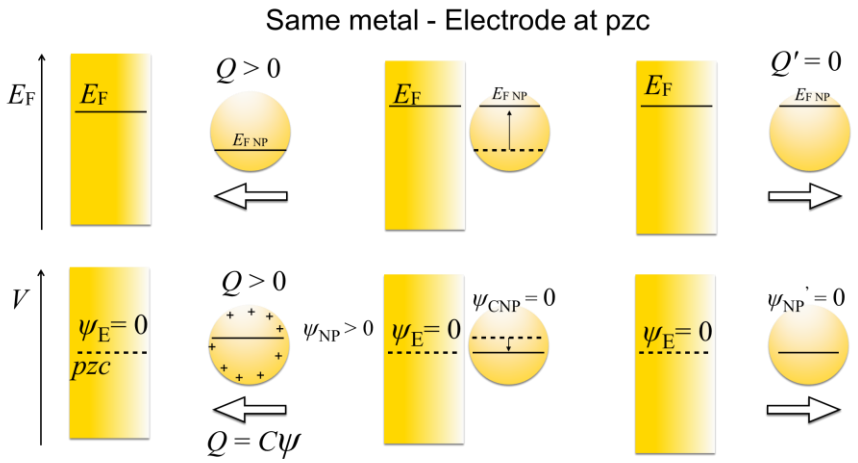

Scheme S1. Electrode and NP made of the same metal. Top panel: Fermi levels. Bottom panel: potential difference between metal and solution. The electrode is at the common pzc. Before collision, the NP is positively charged and, therefore, has a lower Fermi level than the electrode. As the NP capacitance varies with the distance to the electrode, the potential difference between the NP and the solution varies when the NP approaches the electrode. Upon collision the potentials reach the same value, and the NP potential does not change when it moves into the bulk of the solution.

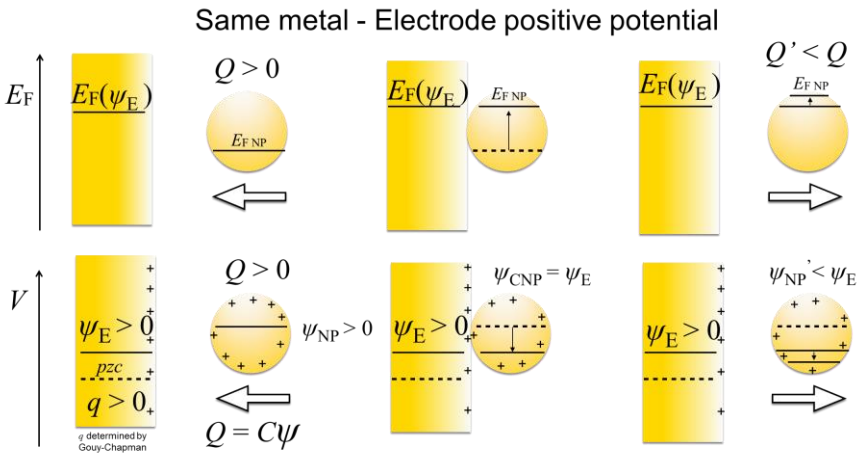

Scheme S2. Similar to Scheme S1, with the electrode at a positive potential. Before collision, the NP is positively charged and has a lower Fermi level than the electrode. As the NP capacitance varies with the distance to the electrode, the potential difference between the NP and the solution varies both when the NP approaches the electrode and when it departs from the electrode after collision

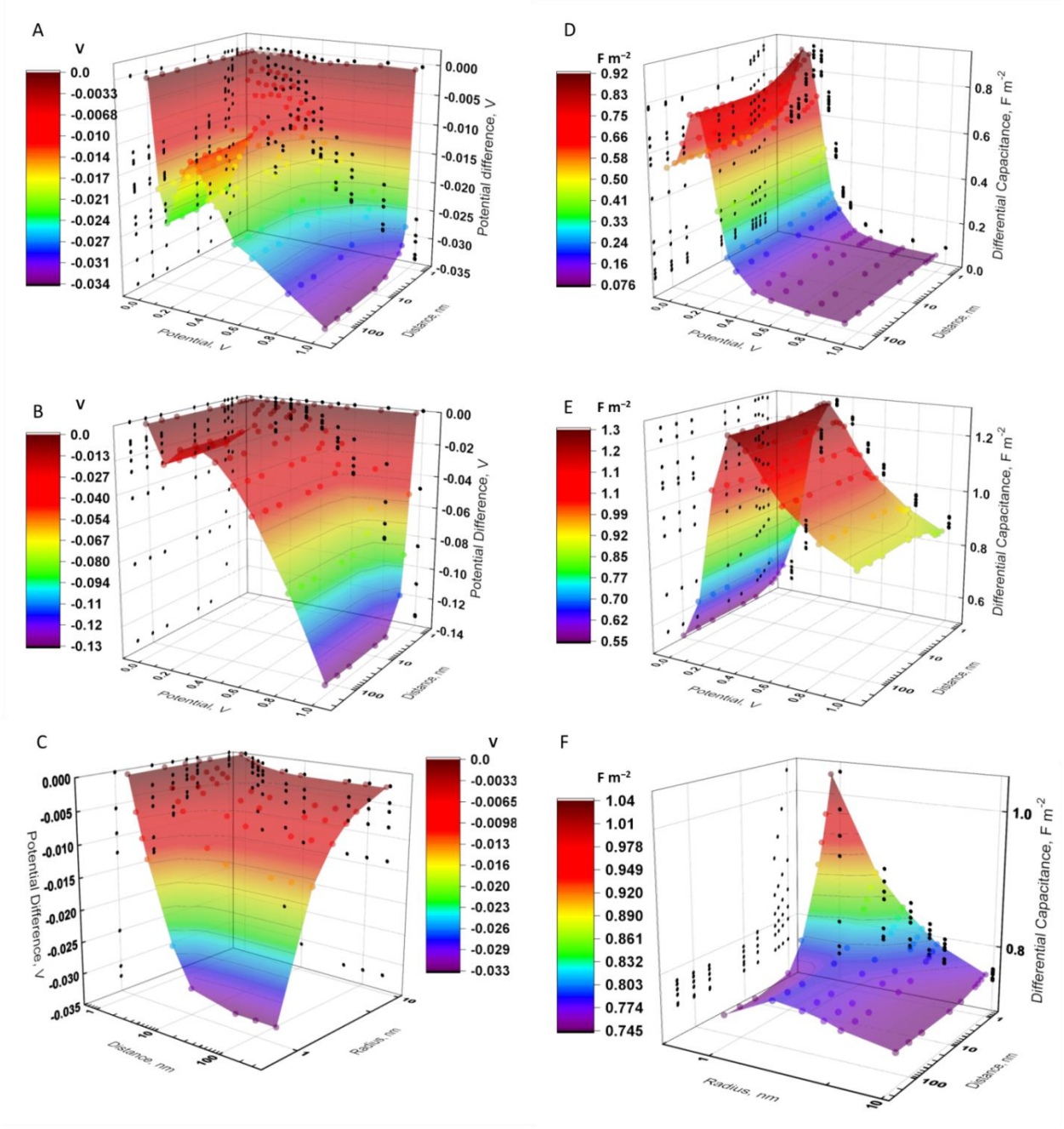

Figure S3. Potential difference between the NP and the electrode after collision as a function of the NP distance and electrode potential for $R_{\mathrm{NP}} = 2\,\mathrm{nm}$, calculated: A) with $\varepsilon_{\mathrm{r}} = 78$ (model I) and B) with the Booth model for the relative permittivity (model II). C) Effect of the NP radius on the differential capacitance at 0.2 V calculated with the Booth model. Differential capacitance at the electrode potential as a function of the NP distance and electrode potential for $R_{\mathrm{NP}} = 2\,\mathrm{nm}$, calculated: D) with $\varepsilon_{\mathrm{r}} = 78$ (model I) and E) with the Booth model for the relative permittivity (model II). F) Effect of the NP radius on the differential capacitance at 0.2 V calculated with the Booth model.

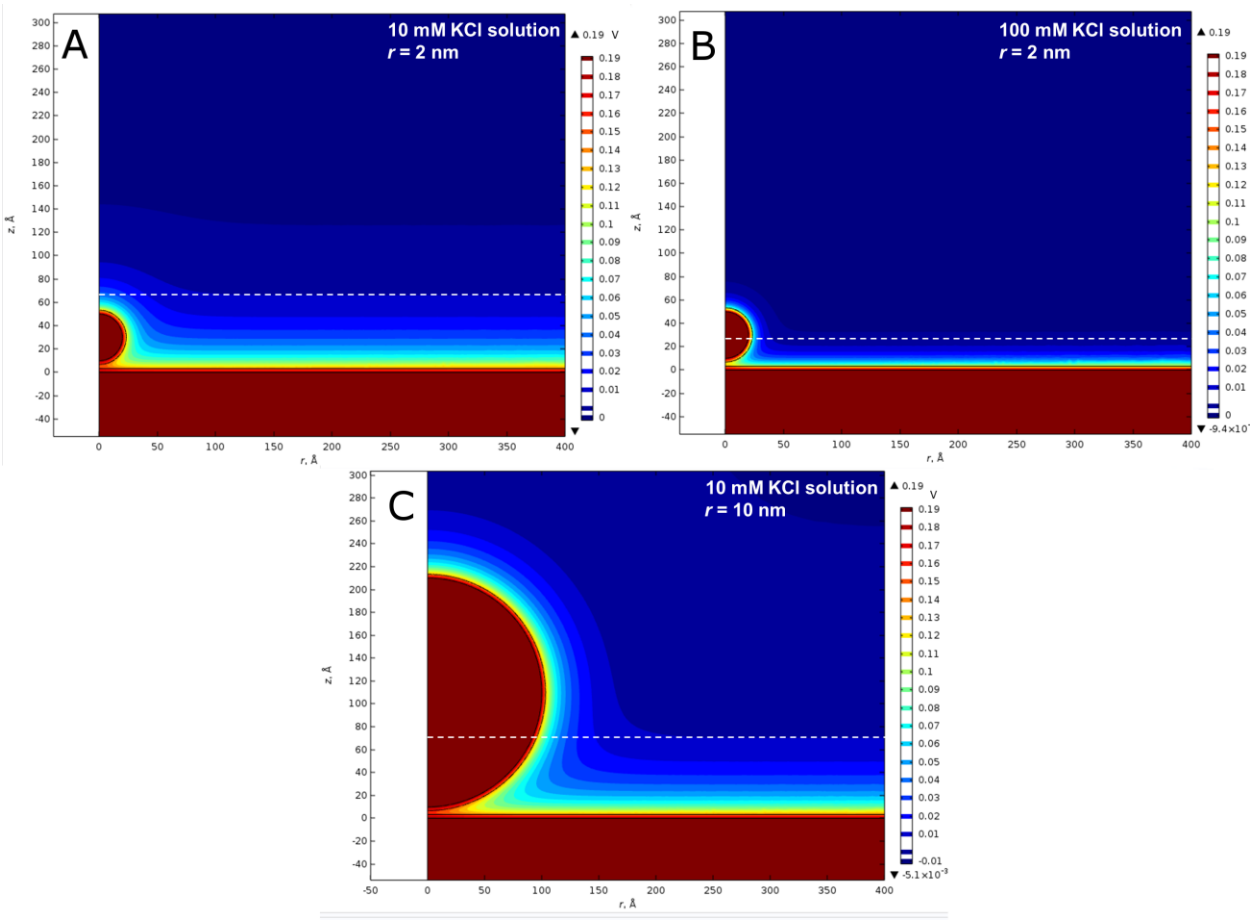

Figure S4. The immersion of the NP in the electric double layer of the electrode at 0.2 V. Small NPs (R = 2 nm) are completely immersed in the double layer in dilute electrolyte solutions (A), but the thickness of the double layer decreases in more concentrated electrolyte solutions (B). The effect of the electric double layer is smaller on larger particles, as they only partially feel the effects of the double layer even in dilute electrolyte solutions (C). s = 1 nm, calculated with Model II. All assuming no specific adsorption of chloride.

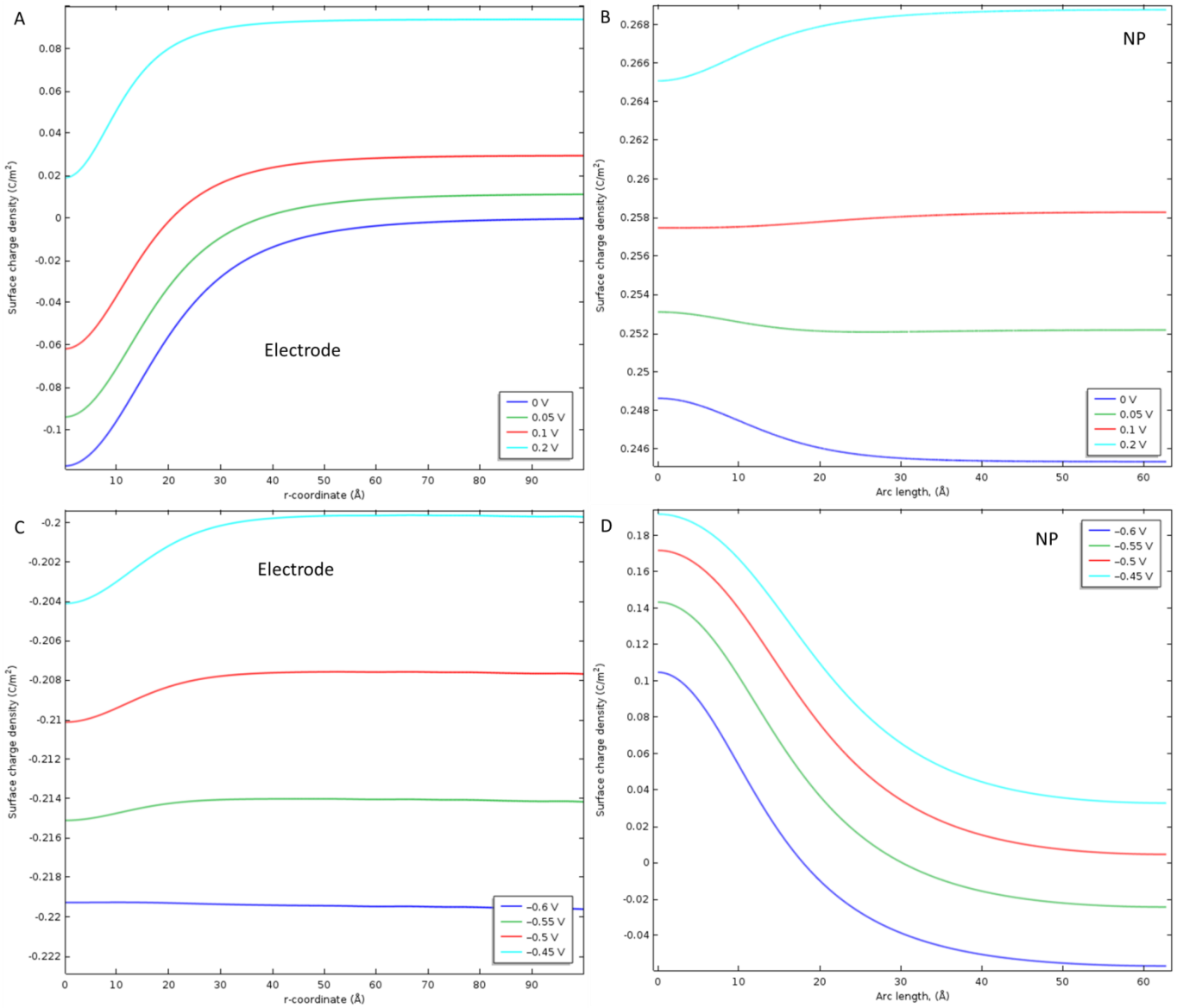

Figure S5. Surface charge densities of the electrode (A, C) and the NP (B, D) for $-E_{\mathrm{pzc}} = 0.5\mathrm{V}$, for the electrode potentials where the repulsive force changes to attractive (A, B) and again to repulsive (C, D). R_{NP} = 2 nm, s = 1 nm, calculated with model II.

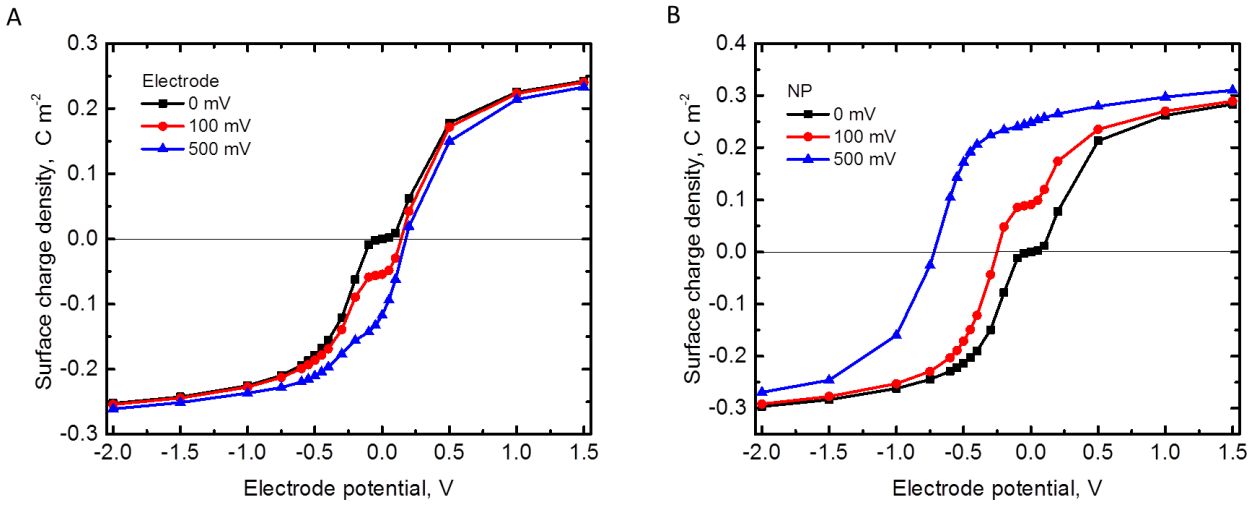

Figure S6. Surface charge density of the electrode at the point closest to the NP (r = 0, z = 0) (A) and the surface charge density at the NP surface at the point closest to the electrode (r = 0, z = 10 Å) (B), as the function of electrode potential, for $-E_{\mathrm{pzc}}$ values of 0, 100 and 500 mV. R_{NP} = 2 nm, s = 1 nm, calculated with model II.

3. Approximate solution of the PBE for a spherical NP with a Stern layer

The main text includes an approximate solution of the PBE for an isolated spherical NP in electrolyte solution with the aim of discussing its differential capacitance. For the sake of simplicity, the approximation discussed is of intermediate complexity. We comment here some details of this approximation as well as another, more accurate approximation. To the best of our knowledge, there are no approximated solutions of the PBE modified to include finite ion size and dielectric saturation effects outside a spherical NP. The results presented in the main text are based on the exact numerical solution of the modified PBE and not in the approximations here discussed for the classical PBE.

The potential distribution inside the Stern layer is

$$\varphi(r) = \varphi(R_{\mathrm{NP}}) + \frac{zF\sigma R_{\mathrm{NP}}}{\varepsilon_0 \varepsilon_{\mathrm{r}} RT}\left(\frac{R_{\mathrm{NP}}}{r} - 1\right) \quad , R_{\mathrm{NP}} \le r \le R_{\mathrm{NP}} + \delta \, . \tag{PBE1}$$

Outside this layer the PBE is approximated by[PBE1]

$$\varphi'' = -\frac{2}{r}\varphi' + \kappa^2 \sinh\varphi \approx \frac{4\kappa}{R_{\mathrm{NP}} + \delta}\sinh\frac{\varphi}{2} + \kappa^2 \sinh\varphi \quad , \; r \ge R_{\mathrm{NP}} + \delta \, . \tag{PBE2}$$

and integrated with the boundary conditions $\varphi = 0$ and $\varphi' = 0$ when $\kappa r \to \infty$ to yield

$$\frac{1}{\kappa}\varphi' \approx -2\sinh\frac{\varphi}{2}\left[1+\frac{2}{\kappa(R_{\rm NP}+\delta)}\operatorname{csch}^2\frac{\varphi}{4}\right]^{1/2} \approx -2\sinh\frac{\varphi}{2}-\frac{4}{\kappa(R_{\rm NP}+\delta)}\tanh\frac{\varphi}{4}. \qquad \text{(PBE3)}$$

The boundary condition $\varphi'(R_{\rm NP}+\delta) = -zF\sigma/[\varepsilon_0\varepsilon_{\rm r}RT(1+\delta/R_{\rm NP})^2]$ then gives

$$\begin{aligned}\sigma &\approx \frac{\varepsilon_0\varepsilon_{\rm r}\kappa RT(1+\delta/R_{\rm NP})^2}{zF}\left[2\sinh\frac{\varphi(R_{\rm NP}+\delta)}{2}+\frac{4}{\kappa(R_{\rm NP}+\delta)}\tanh\frac{\varphi(R_{\rm NP}+\delta)}{4}\right] \\ &= \frac{\varepsilon_0\varepsilon_{\rm r}RT}{zF}\frac{1+\delta/R_{\rm NP}}{R_{\rm NP}}\left[2\kappa(R_{\rm NP}+\delta)\sinh\frac{\varphi(R_{\rm NP}+\delta)}{2}+4\tanh\frac{\varphi(R_{\rm NP}+\delta)}{4}\right]\end{aligned} \qquad \text{(PBE4)}$$

from which the differential capacitance of the NP and the potential drop in the Stern layer can be evaluated as

$$\begin{aligned}C_{\rm NP}(R_{\rm NP}+\delta) &\equiv 4\pi R_{\rm NP}^2\frac{zF}{RT}\frac{{\rm d}\sigma}{{\rm d}\varphi(R_{\rm NP}+\delta)} \\ &= 4\pi\varepsilon_0\varepsilon_{\rm r}(R_{\rm NP}+\delta)\left[\kappa(R_{\rm NP}+\delta)\cosh\frac{\varphi(R_{\rm NP}+\delta)}{2}+\operatorname{sech}^2\frac{\varphi(R_{\rm NP}+\delta)}{4}\right]\end{aligned} \qquad \text{(PBE5)}$$

$$\begin{aligned}\varphi(R_{\rm NP})-\varphi(R_{\rm NP}+\delta) &= \frac{zF\sigma}{\varepsilon_0\varepsilon_{\rm r}RT}\frac{R_{\rm NP}}{R_{\rm NP}+\delta} \\ &= \frac{2\delta}{R_{\rm NP}}\left[\kappa(R_{\rm NP}+\delta)\sinh\frac{\varphi(R_{\rm NP}+\delta)}{2}+2\tanh\frac{\varphi(R_{\rm NP}+\delta)}{4}\right]\end{aligned} \qquad \text{(PBE6)}$$

which are used in the main text.

A more accurate approximate solution of the PBE outside the Stern layer is [PBE1]

$$\varphi(r) = 4\,\mathrm{artanh}\,Bs + 4\,\mathrm{artanh}\frac{Bs}{1+2\kappa(R_{\rm NP}+\delta)} \quad \text{or}$$

$$\tanh\frac{\varphi(r)}{4} = 2Bs\frac{1+\kappa(R_{\rm NP}+\delta)}{1+2\kappa(R_{\rm NP}+\delta)+B^2s^2} \qquad \text{(PBE7)}$$

where

$$s \equiv \frac{R_{\rm NP}+\delta}{r}\exp[-\kappa(r-R_{\rm NP}-\delta)] \qquad \text{(PBE8)}$$

and B is determined as a function $\varphi(R_{\rm NP}+\delta)$ of by solving the algebraic equation

$$\tanh\frac{\varphi(R_{\rm NP}+\delta)}{4} = 2B\frac{1+\kappa(R_{\rm NP}+\delta)}{1+2\kappa(R_{\rm NP}+\delta)+B^2}. \qquad \text{(PBE9)}$$

The surface charge density is then obtained as [PBE1]

$$\sigma \approx \frac{\varepsilon_0\varepsilon_r RT(1+\delta/R_{NP})^2}{zF}\varphi'(R_{NP}+\delta) = \\ = \frac{2\varepsilon_0\varepsilon_r RT}{zF}(1+\delta/R_{NP})^2 \sinh\frac{\varphi(R_{NP}+\delta)}{2} \\ \times\left[1+\frac{2}{\kappa(R_{NP}+\delta)}\operatorname{sech}^2\frac{\varphi(R_{NP}+\delta)}{4}+\frac{8}{\kappa^2(R_{NP}+\delta)^2}\frac{\ln\left(\cosh\frac{\varphi(R_{NP}+\delta)}{4}\right)}{\sinh^2\frac{\varphi(R_{NP}+\delta)}{2}}\right]^{1/2} \quad \text{(PBE10)}$$

and the potential drop in the Stern layer is

$$\varphi(R_{NP})-\varphi(R_{NP}+\delta) = \frac{zF\sigma}{\varepsilon_0\varepsilon_r RT}\frac{R_{NP}\delta}{R_{NP}+\delta}. \quad \text{(PBE11)}$$

4. Force between charged plates (PP) at different potentials separated by a *z*:*z* electrolyte solution

In a *z*:*z* electrolyte the Poisson-Boltzmann equation (PBE), eqn (4), can be multiplied by $2\nabla\varphi$ and integrated to give

$$(\nabla\varphi)^2 = 2\kappa^2(\cosh\varphi - B) \quad \text{(PP1)}$$

where B is an integration constant. To describe the interaction between two parallel plates, we note that $\Pi(z)-\varepsilon_0\varepsilon_r E_z^2(z)/2$ is independent of the position between the plates, where $\Pi(z)=2RTc^b[\cosh\varphi(z)-1]$ is the local osmotic pressure measured with respect to its bulk value. The local electric field, eqn (PP2), satisfies

$$E_z^2(z) = \left(\frac{RT}{zF}\right)^2 2\kappa^2[\cosh\varphi(z)-B] = \frac{4RTc^b}{\varepsilon_0\varepsilon_r}[\cosh\varphi(z)-B] \quad \text{(PP2)}$$

where we have used $\varepsilon_0\varepsilon_r\kappa^2(RT/zF)^2 = 2RTc^b$. As required by the mechanical equilibrium, the total stress

$$\Pi(z)-\frac{1}{2}\varepsilon_0\varepsilon_r E_z^2(z) = 2RTc^b(B-1) \quad \text{(PP3)}$$

is indeed independent of position. Therefore, the force on a plate can be determined by evaluating the integration constant *B* in eqn (PP1) from the values of the potential at the plates and their separation.

The integration of eqn (PP1) in planar geometry under arbitrary boundary conditions can be done analytically but involves elliptic integrals or Jacobi elliptic functions.[PP1,PP2] To avoid these complications, it is customary to discuss the interaction between plates using the classical HHF method for the small potentials.[PP3] Consider that the plate located at $z = 0$ has potential φ_{NP} and the plate at $z = s$ has potential φ_{E}. For the sake of simplicity, these dimensionless potentials are both small so that the PBE can be linearized to $\mathrm{d}^2\varphi/\mathrm{d}z^2 = \kappa^2\varphi$. The solution of this equation is

$$\varphi(z) = \varphi_{\mathrm{NP}}\cosh(\kappa z) + \left[\frac{\varphi_{\mathrm{E}}}{\sinh(\kappa s)} - \frac{\varphi_{\mathrm{NP}}}{\tanh(\kappa s)}\right]\sinh(\kappa z)\,. \tag{PP4}$$

Then, the electric field is

$$\frac{1}{\kappa}\frac{\mathrm{d}\varphi}{\mathrm{d}z} = \frac{\varphi_{\mathrm{E}}\cosh(\kappa z) - \varphi_{\mathrm{NP}}\cosh[\kappa(z-s)]}{\sinh(\kappa s)} \tag{PP5}$$

and the constant B is given by

$$2(B-1) = 2\cosh\varphi - 2 - \left(\frac{1}{\kappa}\frac{\mathrm{d}\varphi}{\mathrm{d}z}\right)^2 \approx \varphi^2 - \left(\frac{1}{\kappa}\frac{\mathrm{d}\varphi}{\mathrm{d}z}\right)^2 = \left(\frac{\varphi_{\mathrm{NP}}+\varphi_{\mathrm{E}}}{2\cosh(\kappa s/2)}\right)^2 - \left(\frac{\varphi_{\mathrm{NP}}-\varphi_{\mathrm{E}}}{2\sinh(\kappa s/2)}\right)^2. \tag{PP6}$$

Thus, we conclude that the total force

$$F(s) = 2RTc^{\mathrm{b}}(B-1)A, \tag{PP7}$$

where A is the plate area, is positive (i. e., repulsive) when $\varphi_{\mathrm{NP}} = \varphi_{\mathrm{E}}$, but it can be attractive when the separation s between the plates is small and their potentials are different, even if they are of the same sign.[PP4,PP5] Consider, without loss of generality, that $\varphi_{\mathrm{NP}} > \varphi_{\mathrm{E}} > 0$. The force reverses from repulsive to attractive when $\tanh(\kappa s/2) = (\varphi_{\mathrm{NP}} - \varphi_{\mathrm{E}})/(\varphi_{\mathrm{NP}} + \varphi_{\mathrm{E}})$, that is, when $\varphi_{\mathrm{E}} = \varphi_{\mathrm{NP}}\,\mathrm{e}^{-\kappa s}$; this is consistent with the arguments made above, as the condition $\varphi_{\mathrm{E}} = 4\mathrm{artanh}[\tanh(\varphi_{\mathrm{NP}}/4)\exp(-\kappa s)]$ for vanishing force mentioned at the beginning of this section corresponds to $\varphi_{\mathrm{E}} \approx \varphi_{\mathrm{NP}}\,\mathrm{e}^{-\kappa s}$ for small potentials. The force between the plates is attractive if $\varphi_{\mathrm{E}} < \varphi_{\mathrm{NP}}\,\mathrm{e}^{-\kappa s}$ and repulsive if $\varphi_{\mathrm{NP}} > \varphi_{\mathrm{E}} > \varphi_{\mathrm{NP}}\,\mathrm{e}^{-\kappa s}$.

The attractive interaction between plates with dissimilar potentials of the same sign corresponds to an attractive interaction between charges densities of opposite sign.[PP6,PP7] The plates have opposite charge densities when $\varphi_{\mathrm{NP}} > \varphi_{\mathrm{E}}\cosh(\kappa s)$, and hence the condition $\varphi_{\mathrm{NP}} > \varphi_{\mathrm{E}}\,\mathrm{e}^{\kappa s}$ for observing an attractive force implies that the plates bear charge densities of opposite sign as $\mathrm{e}^{\kappa s} = \cosh(\kappa s) + \sinh(\kappa s) > \cosh(\kappa s)$. Indeed, the charge density on the plate at $z = 0$ is

$$\sigma_{\mathrm{NP}} = -\varepsilon_0\varepsilon_{\mathrm{r}}\kappa\frac{RT}{zF}\frac{\mathrm{d}\varphi}{\mathrm{d}z}\bigg|_{z=0} = \varepsilon_0\varepsilon_{\mathrm{r}}\kappa\frac{RT}{zF}\frac{\varphi_{\mathrm{NP}}\cosh(\kappa s)-\varphi_{\mathrm{E}}}{\sinh(\kappa s)}$$
$$= \varepsilon_0\varepsilon_{\mathrm{r}}\kappa\frac{RT}{2zF}\left[(\varphi_{\mathrm{NP}}+\varphi_{\mathrm{E}})\tanh(\kappa s/2)+\frac{\varphi_{\mathrm{NP}}-\varphi_{\mathrm{E}}}{\tanh(\kappa s/2)}\right] > 0 \qquad \text{(PP8)}$$

and the charge density on the plate at z = s is

$$\sigma_{\mathrm{E}} = \varepsilon_0\varepsilon_{\mathrm{r}}\kappa\frac{RT}{zF}\frac{\mathrm{d}\varphi}{\mathrm{d}z}\bigg|_{z=s} = \varepsilon_0\varepsilon_{\mathrm{r}}\kappa\frac{RT}{zF}\frac{\varphi_{\mathrm{E}}\cosh(\kappa s)-\varphi_{\mathrm{NP}}}{\sinh(\kappa s)}$$
$$= \varepsilon_0\varepsilon_{\mathrm{r}}\kappa\frac{RT}{2zF}\left[(\varphi_{\mathrm{NP}}+\varphi_{\mathrm{E}})\tanh(\kappa s/2)-\frac{\varphi_{\mathrm{NP}}-\varphi_{\mathrm{E}}}{\tanh(\kappa s/2)}\right]. \qquad \text{(PP9)}$$

The latter vanishes when $\varphi_{\mathrm{NP}} = \varphi_{\mathrm{E}}\cosh(\kappa s)$. Then, the plates have charge densities of opposite sign when $\varphi_{\mathrm{NP}} > \varphi_{\mathrm{E}}\cosh(\kappa s)$. For fixed φ_{E} and φ_{NP}, the repulsive force is maximum at a separation such that $\varphi_{\mathrm{NP}} = \varphi_{\mathrm{E}}\cosh(\kappa s)$, which corresponds to vanishing charge density on the plate at z = s.

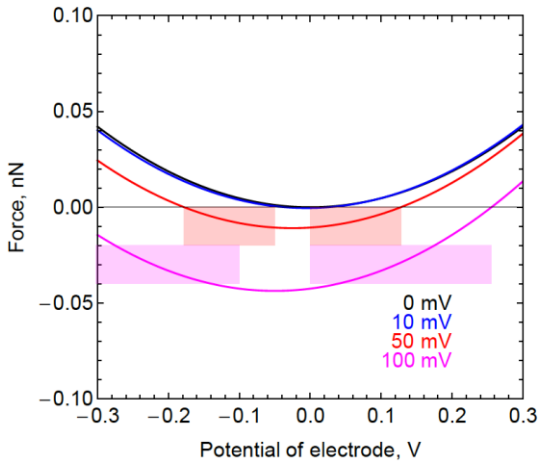

Figure S7. Force $2RTc^{\mathrm{b}}(B-1)A$ between two parallel plates of area $A = \pi R_{\mathrm{NP}}^2$ separated by 1 nm thick layer of a 10 mmol/L 1:1 electrolyte solution. The potential of one plate is indicated in the abscissa axis. Four values (0, 10, 50 and 100 mV) have been considered for the potential difference $(RT/zF)(\varphi_{\mathrm{NP}}-\varphi_{\mathrm{E}})$ between the plates. The shaded regions correspond to ranges of attraction between two plates at potentials of the same sign.

Figure S7 evaluates the force $2RTc^{\mathrm{b}}(B-1)A$ for a typical area A of a 2 nm NP and shows a remarkable agreement with the results shown in Figure 3A-C, which are then partly explained. Moreover, eqn (PP6) explains that repulsion dominates when φ_{NP} and φ_{E} are increased in magnitude while keeping constant $\varphi_{\mathrm{NP}}-\varphi_{\mathrm{E}}$, as observed in Figure 3A-C. Finally, although these results have been derived from the linearized PBE, these conclusions are expected to hold qualitatively for large potentials.

The relation between the surface charge densities and the surface potentials can be presented in matrix form as

$$\begin{pmatrix}\sigma_{\mathrm{NP}}\\ \sigma_{\mathrm{E}}\end{pmatrix}=\varepsilon_0\varepsilon_{\mathrm{r}}\kappa\begin{pmatrix}\coth(\kappa s) & -\operatorname{csch}(\kappa s)\\ -\operatorname{csch}(\kappa s) & \coth(\kappa s)\end{pmatrix}\begin{pmatrix}\psi_{\mathrm{NP}}\\ \psi_{\mathrm{E}}\end{pmatrix}. \tag{PP10}$$

At large separations, $\kappa s >> 1$, there is no mutual influence and the areal capacitance of the isolated plates is $C_{\mathrm{GC}\infty}=\varepsilon_0\varepsilon_{\mathrm{r}}\kappa$. In general, the areal capacitance of one plate, $C_{\mathrm{NP}}(s)=\left(\partial\sigma_{\mathrm{NP}}/\partial\psi_{\mathrm{NP}}\right)_{s,\psi_{\mathrm{E}}}$ $=\varepsilon_0\varepsilon_{\mathrm{r}}\kappa\coth(\kappa s)$, is a decreasing function of *s*.

When the plates interact at constant potentials, the (surface density of) potential energy is

$$\begin{aligned}\tilde{W}(s)&=-\frac{1}{2}\left(\sigma_{\mathrm{NP}}\psi_{\mathrm{NP}}+\sigma_{\mathrm{E}}\psi_{\mathrm{E}}\right)=\frac{\varepsilon_0\varepsilon_{\mathrm{r}}\kappa}{2}\left[2\psi_{\mathrm{NP}}\psi_{\mathrm{E}}\operatorname{csch}(\kappa s)-\left(\psi_{\mathrm{NP}}^2+\psi_{\mathrm{E}}^2\right)\coth(\kappa s)\right]\\&=-\frac{\varepsilon_0\varepsilon_{\mathrm{r}}\kappa}{4}\left[(\psi_{\mathrm{NP}}+\psi_{\mathrm{E}})^2\tanh(\kappa s/2)+(\psi_{\mathrm{NP}}-\psi_{\mathrm{E}})^2\coth(\kappa s/2)\right]\end{aligned} \tag{PP11}$$

and its derivative gives the force $F(s)$ between the plates

$$\begin{aligned}\frac{F(s)}{A}&=-\frac{\mathrm{d}\tilde{W}}{\mathrm{d}s}=\frac{\varepsilon_0\varepsilon_{\mathrm{r}}\kappa^2}{2}\left[\left(\frac{\psi_{\mathrm{NP}}+\psi_{\mathrm{E}}}{2\cosh(\kappa s/2)}\right)^2-\left(\frac{\psi_{\mathrm{NP}}-\psi_{\mathrm{E}}}{2\sinh(\kappa s/2)}\right)^2\right]\\&=RTc^{\mathrm{b}}\left[\left(\frac{\varphi_{\mathrm{NP}}+\varphi_{\mathrm{E}}}{2\cosh(\kappa s/2)}\right)^2-\left(\frac{\varphi_{\mathrm{NP}}-\varphi_{\mathrm{E}}}{2\sinh(\kappa s/2)}\right)^2\right].\end{aligned} \tag{PP12}$$

By subtracting the energy of the isolated plates, the interaction energy is[PP3,PP8]

$$\begin{aligned}\tilde{W}_{\mathrm{int}}&=-\frac{1}{2}\left(\sigma_{\mathrm{NP}}\psi_{\mathrm{NP}}+\sigma_{\mathrm{E}}\psi_{\mathrm{E}}\right)+\frac{1}{2}\left(\sigma_{\mathrm{NP}\infty}\psi_{\mathrm{NP}}+\sigma_{\mathrm{E}\infty}\psi_{\mathrm{E}}\right)\\&=\frac{\varepsilon_0\varepsilon_{\mathrm{r}}\kappa}{2}\left\{\left(\psi_{\mathrm{NP}}^2+\psi_{\mathrm{E}}^2\right)[1-\coth(\kappa s)]+2\psi_{\mathrm{NP}}\psi_{\mathrm{E}}\operatorname{csch}(\kappa s)\right\}\end{aligned} \tag{PP13}$$

where $\sigma_{\mathrm{E}\infty}=C_{\mathrm{GC}\infty}\psi_{\mathrm{E}}$ and $\sigma_{\mathrm{NP}\infty}=C_{\mathrm{GC}\infty}\psi_{\mathrm{NP}}$ are surface charge densities corresponding to infinite separation.

The linear PBE should not be used to describe the interaction at constant charge for small separations, as the potentials may take then so large values that the PBE cannot be linearized.[PP9]

5. Force between a spherical NP and a planar electrode (SP) at constant potentials in an electrolyte solution

Consider a spherical NP and a planar electrode at a separation s in an electrolyte solution with Debye parameter κ. For large particles ($\kappa R_{\mathrm{NP}} >> 1$) and low potentials ($\varphi << 1$), the interaction potential energy between the NP and the electrode when they are hold at constant potentials is[PP3,SP1]

$$W_{\mathrm{int}}^{\psi}(s) = \frac{C_{\infty}}{4}\left[(\psi_{\mathrm{NP}} + \psi_{\mathrm{E}})^2 \ln\left(1+\mathrm{e}^{-\kappa s}\right) + (\psi_{\mathrm{NP}} - \psi_{\mathrm{E}})^2 \ln\left(1-\mathrm{e}^{-\kappa s}\right)\right] \tag{SP1}$$

where $C_{\infty} = 4\pi\varepsilon_0\varepsilon_{\mathrm{r}}R_{\mathrm{NP}}$ is the capacitance of an isolated NP in the absence of electrolyte. Observe that W_{int}^{ψ} is the sum of a positive term proportional to the square of the average potential which describes the potential energy of the NP-electrode system when it is charged as a whole and a negative term proportional to the square of the potential difference that describes the potential energy of a capacitor that uses the NP and the electrode as its "plates".[SP2]

When the NP and the electrode interact at constant potentials, their potential energy is

$$\begin{aligned} W^{\psi}(s) &= -\frac{1}{2}\left(Q_{\mathrm{NP}}\psi_{\mathrm{NP}} + Q_{\mathrm{E}}\psi_{\mathrm{E}}\right) = W_{\mathrm{int}}^{\psi}(s) - \frac{1}{2}\left(C_{\infty}\psi_{\mathrm{NP}}^2 + C_{\mathrm{GC}\infty}A\psi_{\mathrm{E}}^2\right) \\ &= \frac{C_{\infty}}{4}\left[(\psi_{\mathrm{NP}}^2 + \psi_{\mathrm{E}}^2)\ln\left(1-\mathrm{e}^{-2\kappa s}\right) + 2\psi_{\mathrm{NP}}\psi_{\mathrm{E}}\ln\frac{1+\mathrm{e}^{-\kappa s}}{1-\mathrm{e}^{-\kappa s}}\right] - \frac{1}{2}\left(C_{\infty}\psi_{\mathrm{NP}}^2 + C_{\mathrm{GC}\infty}A\psi_{\mathrm{E}}^2\right) \\ &= -\frac{1}{2}\left(C_{\mathrm{NP,NP}}\psi_{\mathrm{NP}}^2 + C_{\mathrm{E,E}}\psi_{\mathrm{E}}^2 + 2C_{\mathrm{NP,E}}\psi_{\mathrm{NP}}\psi_{\mathrm{E}}\right) \end{aligned} \tag{SP2}$$

where in the last step we have introduced the capacitance matrix coefficients and $C_{\mathrm{GC}\infty} = \varepsilon_0\varepsilon_{\mathrm{r}}\kappa$. The charge on the NP is

$$Q_{\mathrm{NP}}(s) = C_{\mathrm{NP,NP}}\psi_{\mathrm{NP}} + C_{\mathrm{NP,E}}\psi_{\mathrm{E}} = C_{\infty}\left[1 - \frac{1}{2}\ln\left(1-\mathrm{e}^{-2\kappa s}\right)\right]\psi_{\mathrm{NP}} - \frac{C_{\infty}}{2}\ln\frac{1+\mathrm{e}^{-\kappa s}}{1-\mathrm{e}^{-\kappa s}}\psi_{\mathrm{E}}. \tag{SP3}$$

The force between the NP and the electrode is

$$F(s) = -\frac{\mathrm{d}W_{\mathrm{int}}^{\psi}}{\mathrm{d}s} = \frac{C_{\infty}\kappa}{4}\left[\frac{(\psi_{\mathrm{NP}} + \psi_{\mathrm{E}})^2}{\mathrm{e}^{\kappa s}+1} - \frac{(\psi_{\mathrm{NP}} - \psi_{\mathrm{E}})^2}{\mathrm{e}^{\kappa s}-1}\right] \tag{SP4}$$

where the first term describes a repulsive contribution and the second one an attractive contribution that dominates at short separations, i.e. if $\mathrm{e}^{\kappa s} < (\psi_{\mathrm{NP}}^2 + \psi_{\mathrm{E}}^2)/2\psi_{\mathrm{NP}}\psi_{\mathrm{E}}$. The similarity between eqns (PP6) and (SP4) is not casual, as the force between a sphere and a plane is closely related to the force between two planar surfaces.[SP3,PP8] In the limit of large separations ($\kappa s >> 1$) this force reduces to

$$F_{\infty}(s) \approx C_{\infty}\kappa\psi_{\mathrm{NP}}\psi_{\mathrm{E}}\mathrm{e}^{-\kappa s} \tag{SP5}$$

and in the absence of electrolyte solution the force is attractive and reduces to

$$F_{\kappa\to 0}(s) = -\frac{C_\infty}{4s}(\psi_{\rm NP} - \psi_{\rm E})^2 \tag{SP6}$$

In the case of NPs with smaller radii, i.e. for arbitrary $\kappa R_{\rm NP}$, and low potentials ($\varphi << 1$), the interaction potential energy between the NP and the electrode when they are hold at constant potentials is[PP8]

$$W^*_{\rm int}(s) = W^{\psi}_{\rm int}(s) + W^{\psi}_{\rm int}(s + 2R_{\rm NP}) + \beta(s) - \beta(s + 2R_{\rm NP}) \tag{SP7}$$

where $W^{\psi}_{\rm int}(x)$ is given by eqn (SP1),

$$\beta(x) = \frac{C_\infty}{4\kappa R_{\rm NP}}\left[(\psi_{\rm NP} + \psi_{\rm E})^2 \,{\rm Li}_2(-{\rm e}^{-\kappa x}) + (\psi_{\rm NP} - \psi_{\rm E})^2 \,{\rm Li}_2({\rm e}^{-\kappa x})\right] \tag{SP8}$$

is a correction function defined from the condition $W^{\psi}_{\rm int}(x) = R_{\rm NP}{\rm d}\beta/{\rm d}x$, and ${\rm Li}_2(z) = \sum_{k=1}^{\infty} z^k/k^2$ is a polylogarithm function whose derivative is ${\rm dLi}_2(z)/{\rm d}z = -\ln(1-z)/z$. The force between the NP and the electrode is then

$$\begin{aligned} F^*(s) = -\frac{{\rm d}W^*_{\rm int}}{{\rm d}s} = \frac{C_\infty \kappa}{4}(\psi_{\rm NP} + \psi_{\rm E})^2 \left(\frac{1}{{\rm e}^{\kappa s}+1} + \frac{1}{{\rm e}^{\kappa(s+2R_{\rm NP})}+1} + \frac{1}{\kappa R_{\rm NP}} \ln\frac{{\rm e}^{-\kappa(s+2R_{\rm NP})}+1}{{\rm e}^{-\kappa s}+1}\right) \\ -\frac{C_\infty \kappa}{4}(\psi_{\rm NP} - \psi_{\rm E})^2 \left(\frac{1}{{\rm e}^{\kappa s}-1} + \frac{1}{{\rm e}^{\kappa(s+2R_{\rm NP})}-1} + \frac{1}{\kappa R_{\rm NP}} \ln\frac{{\rm e}^{-\kappa s}-1}{{\rm e}^{-\kappa(s+2R_{\rm NP})}-1}\right). \end{aligned} \tag{SP9}$$

This force is repulsive if $\psi_{\rm NP} = \psi_{\rm E}$, but it can be attractive at short separations if $\psi_{\rm NP} \neq \psi_{\rm E}$. In the limit of large separations ($\kappa s >> 1$) the force reduces to

$$F^*_\infty(s) = C_\infty \kappa \psi_{\rm NP}\psi_{\rm E}{\rm e}^{-\kappa s}\left(1 + {\rm e}^{-2\kappa R_{\rm NP}} + \frac{1-{\rm e}^{-2\kappa R_{\rm NP}}}{\kappa R_{\rm NP}}\right) \tag{SP10}$$

and in the absence of electrolyte solution the force is attractive and reduces to

$$F^*_{\kappa\to 0}(s) = -\frac{C_\infty}{4}(\psi_{\rm NP} - \psi_{\rm E})^2\left[\frac{1}{s} + \frac{1}{s+2R_{\rm NP}} - \frac{\ln(1+2R_{\rm NP}/s)}{R_{\rm NP}}\right]. \tag{SP11}$$

The sphere-plate interaction in electrolyte solutions has been discussed in a number of papers, most of them considering the small potential approximation;[SP4-SP10] the case of metal sphere and metal plate must sometimes be obtained by taking the limit of relative permittivity (of the sphere and the plate) tending to infinity. Ohshima has discussed an exact solution for the plate-sphere interaction that is based on a generalization of the method of image charges.[SP11,SP12] Unfortunately, the expression obtained in terms of series expansions is so complicated that has very limited practical value. The important remark

from Ohshima work, however, is that the image charges always contribute with an attractive term to the interaction force between the sphere and the plate.[SP12]

6. Solution of the Laplace equation (LE) in the sphere-plate capacitor

In the absence of electrolyte the potential distribution satisfies the Laplace equation $\nabla^2\psi = 0$, which can be solved analytically in the space between the conducting surfaces of a sphere-plate capacitor. The electric field distribution is determined by the boundary conditions and the potential is defined up to an arbitrary constant. That is, only the potential difference between the sphere (or nanoparticle NP) and the plate (or electrode E) is relevant. For this reason, the description of the electrostatics of the sphere-plate interaction often considers that the plate is grounded. Should the plate potential be different, its value should be added to the potential distribution described below; with the correct potential difference between sphere and plate. In electrostatics it is well known that for a conducting sphere approaching a conducting plane, the mutual capacitance coefficient is[LE1,LE2] $C_{\mathrm{NP,E}} = -C_{\mathrm{NP,NP}}$ and, therefore, $Q_{\mathrm{NP}} = C_{\mathrm{NP,NP}}\psi_{\mathrm{NP}} + C_{\mathrm{NP,E}}\psi_{\mathrm{E}} = C_{\mathrm{NP,NP}}(\psi_{\mathrm{NP}} - \psi_{\mathrm{E}})$, which is reduced to $Q_{\mathrm{NP}} = C_{\mathrm{NP}}\psi_{\mathrm{NP}}$ if $\psi_{\mathrm{E}} = 0$.

The centre of the NP of radius R_{NP} is located on the Cartesian z axis at $z_{\mathrm{centre}} = s + R_{\mathrm{NP}}$, where *s* is the separation between NP and electrode. Hereinafter, a tilde ~ denotes division by R_{NP}; e. g., $\tilde{s} \equiv s / R_{\mathrm{NP}}$. Using bispherical coordinates (η, θ, ϕ),[LE3, LE4] the surface $\eta = \eta_0(\tilde{s})$ with

$$\eta_0(\tilde{s}) = \operatorname{arcosh}(1+\tilde{s}) = \ln\left[1 + \tilde{s} + (\tilde{s}^2 + 2\tilde{s})^{1/2}\right] \tag{LE1}$$

is spherical and corresponds to the NP surface; obviously, $z_{\mathrm{centre}} = R_{\mathrm{NP}}\cosh\eta_0$. The surface $\eta = 0$ is planar and corresponds to the plate ($z = 0$ in Cartesian coordinates); the origin of coordinates is the plate position closest to the NP. The space between the sphere and the plate is ($0 \le \eta \le \eta_0(\tilde{s})$, $0 \le \theta \le \pi$, $0 \le \phi \le 2\pi$). The interior of the NP is $\eta > \eta_0(\tilde{s})$.

The solution of the Laplace equation is

$$\psi(\tilde{s}, \eta, \theta) = \psi_{\mathrm{NP}}\, 2^{3/2}(\cosh\eta - \cos\theta)^{1/2} \sum_{m=0}^{\infty} \frac{\sinh[(m+1/2)\eta]}{\exp[(2m+1)\eta_0(\tilde{s})] - 1} P_m(\cos\theta) \tag{LE2}$$

The electric field is

$$\mathbf{E} = -\nabla\psi = -\frac{\cosh\eta - \cos\theta}{a(\tilde{s})}\left(\frac{\partial\varphi}{\partial\eta}\mathbf{e}_\eta + \frac{\partial\varphi}{\partial\theta}\mathbf{e}_\theta\right) = -\frac{\cosh\eta - \cos\theta}{a(\tilde{s})}\left(\frac{\partial\varphi}{\partial\eta}\mathbf{e}_\eta - \sin\theta\frac{\partial\varphi}{\partial\cos\theta}\mathbf{e}_\theta\right) \tag{LE3}$$

where

$$\tilde{a}(\tilde{s}) \equiv a / R_{\mathrm{NP}} = \sinh\eta_0 = (\tilde{s}^2 + 2\tilde{s})^{1/2} \tag{LE4}$$

is a scale parameter of the bispherical coordinates. The electric field only has η component at the surfaces of the sphere and the plate, as the field is normal to these conducting surfaces and they are both constant η surfaces, and hence normal to the bispherical unit vector $\mathbf{e}_\eta$; at the plate $\mathbf{e}_\eta$ points in the positive *z* direction and at the NP it points towards the inside of the NP. The η component of the field is

$$E_\eta = -\frac{\psi_{\mathrm{NP}}}{R_{\mathrm{NP}}}\frac{2^{3/2}(\cosh\eta-\cos\theta)^{1/2}}{\sinh\eta_0}\sum_{m=0}^{\infty}\frac{P_m(\cos\theta)}{\exp[(2m+1)\eta_0]-1} \times\left\{\frac{1}{2}\sinh\eta\sinh[(m+1/2)\eta]+(m+1/2)(\cosh\eta-\cos\theta)\cosh[(m+1/2)\eta]\right\}. \quad \text{(LE5)}$$

At the conducting plate (*z* = 0 and $\eta = 0$) the field is

$$E_{\mathrm{plate},z}(\tilde{s},\theta) = -\frac{\psi_{\mathrm{NP}}}{R_{\mathrm{NP}}}\frac{2^{3/2}(1-\cos\theta)^{3/2}}{\sinh\eta_0}\sum_{m=0}^{\infty}\frac{(m+1/2)P_m(\cos\theta)}{\exp[(2m+1)\eta_0]-1} = -\frac{\psi_{\mathrm{NP}}}{R_{\mathrm{NP}}}\frac{8\sin^3(\theta/2)}{(\tilde{s}^2+2\tilde{s})^{1/2}}\sum_{m=0}^{\infty}\frac{(m+1/2)P_m(\cos\theta)}{[1+\tilde{s}+(\tilde{s}^2+2\tilde{s})^{1/2}]^{2m+1}-1} \quad \text{(LE6)}$$

which can be represented (parametrically in θ) against the distance $\rho(\theta) = a/\tan(\theta/2)$ along the plate to the Cartesian origin for any value of the dimensionless separation $\tilde{s} \equiv s/R_{\mathrm{NP}}$. Since the charge density on the plate is $\sigma(\tilde{s},\theta) = \varepsilon_0\varepsilon_{\mathrm{r}}E_{\mathrm{plate},z}$, the total charge on the plate is

$$\begin{aligned} Q_{\mathrm{plate}} &= \varepsilon_0\varepsilon_{\mathrm{r}}\int_0^{\infty}E_{\mathrm{plate},z}\,2\pi\rho\,d\rho = \pi\varepsilon_0\varepsilon_{\mathrm{r}}a^2\int_0^{\pi}E_{\mathrm{plate},z}\frac{\cos(\theta/2)}{\sin^3(\theta/2)}\mathrm{d}\theta \\ &= -\psi_{\mathrm{NP}}\pi\varepsilon_0\varepsilon_{\mathrm{r}}R_{\mathrm{NP}}\sinh\eta_0\sum_{m=0}^{\infty}\frac{8(m+1/2)}{\exp[(2m+1)\eta_0]-1}\int_0^{\pi}P_m(\cos\theta)\cos(\theta/2)\mathrm{d}\theta \\ &= -\psi_{\mathrm{NP}}2C_\infty\sinh\eta_0\sum_{m=0}^{\infty}\frac{1}{\exp[(2m+1)\eta_0]-1} = -C_{\mathrm{NP}}(\tilde{s})\psi_{\mathrm{NP}} \end{aligned} \quad \text{(LE7)}$$

where $C_\infty = 4\pi\varepsilon_0\varepsilon_{\mathrm{r}}R_{\mathrm{NP}}$ is the capacitance of the isolated NP. The capacitance of the NP is then[LE3]

$$C_{\mathrm{NP}}(\tilde{s}) = 2C_\infty\sum_{m=0}^{\infty}\frac{\sinh\eta_0}{\exp[(2m+1)\eta_0]-1} = 2C_\infty(\tilde{s}^2+2\tilde{s})^{1/2}\sum_{m=0}^{\infty}\frac{1}{[1+\tilde{s}+(\tilde{s}^2+2\tilde{s})^{1/2}]^{2m+1}-1} \quad \text{(LE8)}$$

which can be summed analytically in terms of digamma functions.[LE4] The interesting property is that $C_{\mathrm{NP}}(\tilde{s}) > C_\infty$, that is, the charge separation increases as it approaches the electrode when NP and electrode are hold at constant potentials; note that NP and electrode bear charges of equal magnitudes and opposite signs. The value corresponding to a 2 nm radius NP at 1 nm separation from the electrode is $C_{\mathrm{NP}}(0.5) = 1.535C_\infty$. At this separation and shorter, the NP capacitance can be approximated by

$$C_{\mathrm{NP,NP}}(\tilde{s}) = C_{\infty}\left(\gamma + \frac{1}{2}\ln\frac{2}{\tilde{s}}\right) \tag{LE9}$$

where $\gamma = -\psi_0(1)$ is Euler's gamma.[LE5]

At the sphere surface ($\eta = \eta_0(\tilde{s})$) the space charge density is $\sigma = -\varepsilon_0\varepsilon_{\mathrm{r}}E_{\mathrm{NP},\eta}$ and the field is

$$E_{\eta,\mathrm{NP}}(\tilde{s},\theta) = -\frac{\psi_{\mathrm{NP}}}{R_{\mathrm{NP}}}\frac{2^{1/2}(\cosh\eta_0 - \cos\theta)^{3/2}}{\sinh\eta_0} \times\sum_{m=0}^{\infty}\frac{P_m(\cos\theta)}{\exp[(m+1/2)\eta_0]}\left\{\frac{\sinh\eta_0}{2(\cosh\eta_0-\cos\theta)} + (m+1/2)\coth[(m+1/2)\eta_0]\right\}. \tag{LE10}$$

In the absence of electrolyte, the force between the NP and the grounded electrode is always attractive because the induced charge density on the electrode surface has opposite charge to that on the NP. Equation (LE7) clearly shows that a NP with $\psi_{\mathrm{NP}} = 0.5\,\mathrm{V}$ induces a negative charge on a grounded electrode ($\psi_{\mathrm{E}} = 0$). The surface charge density $\sigma = \varepsilon_0\varepsilon_{\mathrm{r}}E_{\mathrm{plate},z}$ on the electrode surface for $s = 1\,\mathrm{nm}$ and $R_{\mathrm{NP}} = 2\,\mathrm{nm}$ is significant over a circular region of radius a few times R_{NP}. Figure S8 shows σ as a function of the distance $\rho = a/\tan(\theta/2)$ to the origin of Cartesian coordinates (i.e. the point of closest approach to the NP). When compared to the surface charge density on Figure S5 for $\psi_{\mathrm{NP}} = 0.5\,\mathrm{V}$ and $\psi_{\mathrm{E}} = 0$, we observe that the charge density on the electrode is around half in the presence of electrolyte, as it should be expected due to the screening of the interaction, but the spatial extension of the distribution of charge on the electrode is similar in the presence and in the absence of electrolyte. Similarly, the charge density on the NP is also around half in the presence of electrolyte, but its spatial distribution is very similar with and without electrolyte.

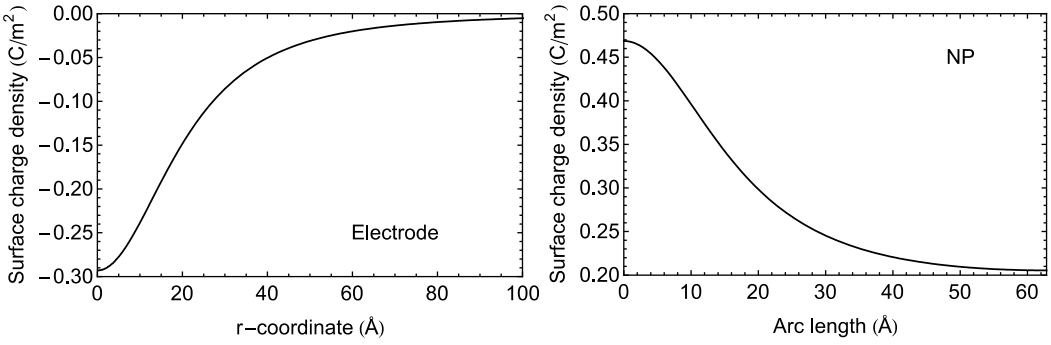

Figure S8. Surface charge densities on a grounded electrode and a 2 nm radius NP at 0.5 V separated by 1 nm in aqueous medium ($\varepsilon_{\mathrm{r}} = 78$) without electrolyte calculated from eqns (LE6) and (LE10).

7. References

JA1 G. Moy, B. Corry, S. Kuyucak and S.-H. Chung, *Biophys. J.* 2000, **78**, 2349–2363, doi: 10.1016/S0006-3495(00)76780-4.

JA2 K. H. Likharev, *Procc. IEEE* 1999, **87**, 606-632, doi: 10.1109/5.752518.

JA3 J. Cervera, J. A. Manzanares, and S. Mafe, *Nanoscale* 2010, **2**, 1033-1038, doi: 10.1039/C0NR00059K.

JA4 J. Cervera, J. A. Manzanares, and S. Mafe, *Nanotechnology* 2009, **20**, 465202, doi: doi:10.1088/0957-4484/20/46/465202.

JA5 T. Laaksonen, V. Ruiz, P. Liljeroth and B. M. Quinn, *Chem. Soc. Rev.* 2008, **37**, 1836–1846, doi: 10.1039/B713681C.

PBE1 H. Ohshima, T. W. Healy and L. R. White, *J. Colloid Interface Sci.*, 1982, **90**, 17–26, doi: 10.1016/0021-9797(82)90393-9.

PP1 D. McCormack, S. L. Carnie and D. Y. C. Chan, *J. Colloid Interface Sci.*, 1995, **169**, 177–196, doi: 10.1006/jcis.1995.1019.

PP2 S. Zhang, *Colloid J.*, 2005, **67**, 554–563, doi:10.1007/s10595-005-0133-1.

PP3 R. Hogg, W. Healy and D. W. Fuertenau, *Trans. Faraday Soc.*, 1966, **62**, 1638–1651, doi: 10.1039/TF9666201638.

PP4 W. B. Russel, D. A. Saville and W. R. Schowalter, *Colloidal Dispersions*, Cambridge University Press, Cambridge, 1989.

PP5 J. H. Masliyah and S. Bhattacharjee, *Electrokinetic and Colloid Transport Phenomena*, John Wiley & Sons, Inc., Hoboken, NJ, USA, 2006.

PP6 B. V. Derjaguin, *Discuss. Faraday Soc*., 1954, **18**, 85–98, doi: 10.1039/DF9541800085.

PP7 F. Evans and H. Wennerström, *The Colloidal Domain: Where Physics, Chemistry, Biology, and Technology Meet*, 2nd ed, Wiley-VCH, New York, 1999, sect 5.1.5.

PP8 S. Lin and M. R. Wiesner, *Langmuir*, 2010, **26**, 16638–16641, doi: 10.1021/la103046w.

PP9 J. Gregory, *J. Colloid Interface Sci.*, 1975, **51**, 44–51, doi:10.1016/0021-9797(75)90081-8.

SP1 S. Bhattacharjee and M. Elimelech, *J. Colloid Interface Sci.*, 1997, **193**, 273–285, doi: 10.1006/jcis.1997.5076.

SP2 P. Peljo, J. A. Manzanares and H. H. Girault, *Langmuir*, 2016, **32**, 5765–5775, doi: 10.1021/acs.langmuir.6b01282.

SP3 Evans, F.; Wennerström , H. The Colloidal Domain: Where Physics, Chemistry, Biology, and Technology Meet, 2nd ed, Wiley-VCH, New York, 1999, ch 5.

SP4 R. J. Phillips, Electrostatic forces between particles and planar interfaces, in Interfacial Forces and Fields. Theory and Applications, Surfactant Science Series 85, J.-P. Hsu (Ed.), Marcel Dekker, New York, ch 6, 251–188.

SP5 H. Ohshima, *J. Colloid Interface Sci.*, 1998, **198**, 42–52, doi: 10.1006/jcis.1997.5240.

SP6 S. L. Carnie, D. Y. C. Chan and J. S. Gunning, *Langmuir*, 1994, **10**, 2993–3009, doi: 10.1021/la00021a024.

SP7 M. L. Grant and D. A. saville, *J. Colloid Interface Sci.*, 1995, **171**, 35–45, doi: 10.1006/jcis.1995.1148.

SP8 J. Ståhlberg, U. Apelgren and B. Jönsson, *J. Colloid Interface Sci.*, 1995, **176**, 397–407, doi: 10.1006/jcis.1995.9952.

SP9 J. Stankovich and S. L. Carnie, *Langmuir*, 1996, **12**, 1453–1461, doi: 10.1021/la00021a024.

SP10 P. Warsynski and Z. Adamczyk, *J. Colloid Interface Sci.*, 1997, **187**, 283–295, doi: 10.1006/jcis.1996.4671.

SP11 H. Ohshima, Interaction of electrical double layers, in Electrical Phenomena at Interfaces, Surfactant Science Series 76, H. Ohshima, K. Furusawa (Eds), Marcel Dekker, New York, 1998, 57-85;

SP12 H. Ohshima, Theory of Colloid and Interfacial Electrical Phenomena, Elsevier, Amsterdam, ch 17.

LE1 W. R. Smythe, *Static and Dynamic Electricity*, 3rd ed rev, Hemisphere Publ., New York, 1989, sect. 5.082.

LE2 E. Durand, *Électrostatique Tome II Problèmes Généraux Conducteurs*, Masson, Paris, 1966, sect. 3.3.4, p. 207.

LE3 M. A. Shallal and J. A. Harrison, *Proc. IEE*, 1969, **116**, 1115–1118, doi: 10.1049/piee.1969.0209.

LE4 S. Banerjee, S. J. McCarty and E. F. Nelsen, "Exact and approximate expressions for the force between a charged conducting sphere and infinite grounded plane", ESA 2015 C4.

LE5 J. Lekner, *J. Electrostatics*, 2011, **69**, 11–14, doi: 10.1016/j.elstat.2010.10.002.